UNIVERSITY OF BIRMINGHAM

Characterisation of PAPSS2 genetic variants *in vitro*

Investigating the role of vitamin D in inflammation related muscle loss

ALIESHA GRIFFIN

August 2011

Centre for Endocrinology Diabetes and Metabolism
School of Clinical and Experimental Medicine
Institute of Biomedical Research
University of Birmingham

UNIVERSITY OF BIRMINGHAM CEDAM

Characterisation of PAPSS2 genetic variants *in vitro*

ALIESHA GRIFFIN

Project One

This project is submitted in partial fulfilment of the requirements for the award of Masters of Medical Research

Centre for Endocrinology Diabetes and Metabolism

School of Clinical and Experimental Medicine

Institute of Biomedical Research

University of Birmingham

August 2011

ABSTRACT

Background: Dehydroepiandrosterone (DHEA) is the precursor for sex steroids in humans and its inactivation by sulphonation is a key regulator of active DHEA levels. Sulphonation of DHEA is controlled by the enzyme SULT2A1, which requires the presence of 3'-phosphoadenosine-5'-phospho-sulphate (PAPS) for activity. In humans PAPS is produced by two isozymes, PAPSS1 and PAPSS2. Several variants of human PAPSS2 are associated with changes in functional activity and have been described in patients presenting with hyperandrogenism and severe bone phenotypes.

Aims: The aim of this project was to characterise the functional activity of hsPAPSS2a genetic variants E10K, M281L and E332K within the DHEA sulphonation pathway.

Methods: The hsPAPSS2a variants were overexpressed in HEK293 cells in conjunction with hsSULT2A1. The capacity of the hsPAPSS2a variants to generate PAPS was determined by the ability of the co-expressed SULT2A1 to convert 3H-DHEA to 3H-DHEAS. The steroids were extracted and thin layer chromatography was used to determine the amount of DHEA conversion.

Results: The novel hsPAPSS2a E332G variant was observed to have a reduction of 50% in functional activity. The hsPAPSS2a E10K and M281L variants showed no significant changes in the DHEA sulphonation pathway.

Conclusions: The clinical recommendation from this study is that patients presenting with androgen excess should be screened for the hsPAPSS2a E332G mutation.

ACKNOWLEDGEMENT

I would like to thank my supervisor Dr. Vivek Dhir for giving me continued direction and assistance throughout this study. I am also indebted to Prof. Wiebke Arlt for her valuable guidance and continued support during this year. I would also like to acknowledge Dr. Jan Idkowiak, Dr. Iwona Bujalska, Dr. Edson Nogeira and Miss Pushpa Patel for their patience, assistance with experiments and helpful advice during this project.

TABLE OF CONTENTS

1 INTRODUCTION 1

1.1 Steroidogenesis 1

1.1.1 Sex steroid synthesis 3

1.2 DHEA and DHEAS 5

1.3 Sulphonation 6

1.4 Sulphotransferases 7

1.5 PAPS 9

1.6 PAPS Synthases 10

1.7 PAPSS2 Genetic Variants 13

2 PROJECT AIMS 16

3 MATERIALS AND METHODS 17

3.1 Molecular Biology 17

3.1.1 Transformation of E. Coli by Heat Shock 17

3.1.2 Plasmid DNA preparation 17

3.1.3 Quantification of Nucleic Acids 18

3.1.4 Site Directed Mutagenesis 19

3.1.5 DNA sequencing 21

3.1.6 RNA extraction 22

3.1.7 Reverse Transcription 22

3.1.8 Quantitative Real Time PCR 23

3.2 Cellular Biology 24

3.2.1 Mammalian Cell Culture 24

3.2.2 Transfection of Mammalian Cell Lines using FuGENE-HD 24

3.2.3 Transfection of Mammalian Cell Lines using Lipofectamine-2000 25

3.2.4 Protein extraction 25

3.2.5 SDS Poly Acrylamide Gel Electrophoresis 26

3.2.6 Western Blot 26

3.3 Biochemical Analysis 27
3.3.1 DHEA to DHEAS Sulphonation Assay *27*
3.3.2 Extraction of DHEA and DHEAS *28*
3.3.3 Thin Layer Chromatography *28*
4 RESULTS 30
4.1 Site Directed Mutagenesis 30
4.2 *In vitro* analysis of hsPAPSS2a genetic variants 32
4.2.1 mRNA expression analysis of pIRES:hsPAPSS2/hsSULT2A *32*
4.2.2 Functional activity *34*
4.2.3 Protein expression analysis of pIRES:PAPSS2a/SULT2A1 ..... *37*
4.3 *In silco* analysis of PAPSS2 genetic variants 38
4.4 Generation of HEK293 stable cell lines 42
5 DISCUSSION 44
5.1 Characterisation of novel PAPSS2a genetic variants 44
5.2 Characterisation of previously analysed PAPSS2a genetic variants 45
6 CONCLUSIONS AND FUTURE DIRECTIONS 48

LIST OF FIGURES

Figure 1: The three major branches of steroidogenesis in humans. 2
Figure 2: Downstream conversion of DHEA in the zona reticularis 4
Figure 3: Conversion of DHEA to androgens within the gonads . 5
Figure 4: Schematic representation of DHEAS serum levels during life. 6
Figure 5: Schematic depiction of hsPAPSS2a protein structure. 11
Figure 6: Site Direct Mutagenesis methodology 21
Figure 7: pIRES:yhsPAPSS2a/hsSULT2A1 expression plasmid. 30
Figure 8: Confirmation of site directed mutagenesis. 32
Figure 9: Representative TLC plate read out. 35
Figure 10: Functional analysis of PAPSS2a genetic variants. 36
Figure 11: Representative western blots of PAPSS2a genetic variants 38
Figure 12: *In silico* modelling of PAPSS2a genetic variants 41
Figure 13: Transfected HEK293 after selection with geneticin 43

LIST OF TABLES

Table 1: Functional activity and population frequency of PAPSS2a genetic variants 15
Table 2: Site Directed Mutagenesis Oligonucleotides.....19
Table 3: Representative expression of PAPSS2a, SULT2A1 and PAPSS1 33

LIST OF ABBREVIATIONS

3βHSD2	3β-hydroxysteroid dehydrogenase type 2
17βHSD5	17β-hydroxysteroid dehydrogenase type five
APS	adenosine 5´-phosphosulphate
cDNA	complementary DNA
DHEA	dehydroepiandrosterone
DHEAS	dehydroepiandrosterone sulphate
LB media	Luria Bertani media
SULT	sulphotransferases
PAPS	3´-phosphoadenosine 5´- phosphosulfate
PAPSS	3´-phosphoadenosine 5´-phosphosulfate synthase
PBS	phosphate buffered saline
PBST	phosphate buffered saline with 0.1% Tween 20
TLC	Thin layer chromatography

1 INTRODUCTION

1.1 Steroidogenesis

Steroidogenesis is a biochemical process that synthesises active steroid hormones from cholesterol. These hormones are involved in many physiological processes including development, sex determination and maintaining homeostasis throughout life. The sex steroids, mineralocorticoids and glucocorticoids make up the three physiological categories of steroids (Miller and Auchus, 2010). Specifically, sex steroids (androgen and oestrogen) are responsible for the differentiation into male or female during embryonic development, as well as the development of sexual maturation and reproductive functions during adulthood. Glucocorticoids have key roles in maintaining metabolic homeostasis, in addition to initiating the body's stress response. Finally, mineralocorticoids are involved in osmoregulation by controlling the mineral and water balance in the body.

The biosynthesis of steroids involves a complex network of enzymatic reactions. The steroidogenic pathway in humans (Figure 1) is controlled at many levels including the regulation of participating enzymes and cofactors, cellular localisation of substrates and tissue specific pathways. The first step in the biosynthesis of all steroid hormones is the conversion of cholesterol to pregnenolone by CYP11A1 (Miller and Auchus, 2010). Both mouse CYP11A1 knockout (Hu et al., 2002) and rare patients with CYP11A1 mutations (Tajima et al., 2001, Kim et al., 2008) have a failure of steroidogenesis, demonstrating that all biosynthesis of steroids begins with this enzymatic reaction.

The conversion of cholesterol to pregnenolone occurs within the two major sites of steroidogenesis in humans; the adrenal glands and the gonads (Miller and Auchus, 2010). Humans have two adrenal glands which are situated above each kidney and can be divided into the outer cortex and the inner medulla. While epinephrine and norepinephrine are secreted by the medulla, the adrenal cortex is responsible for secretion of steroid hormones. The cortex can be subdivided in to the outer *zona glomerulosa*, the middle *zona fasciculata* and the inner *zona reticularis*, which are responsible for the production of mineralocorticoids, sex steroid precursors and glucocorticoids, respectively (Simpson and Waterman, 1988).

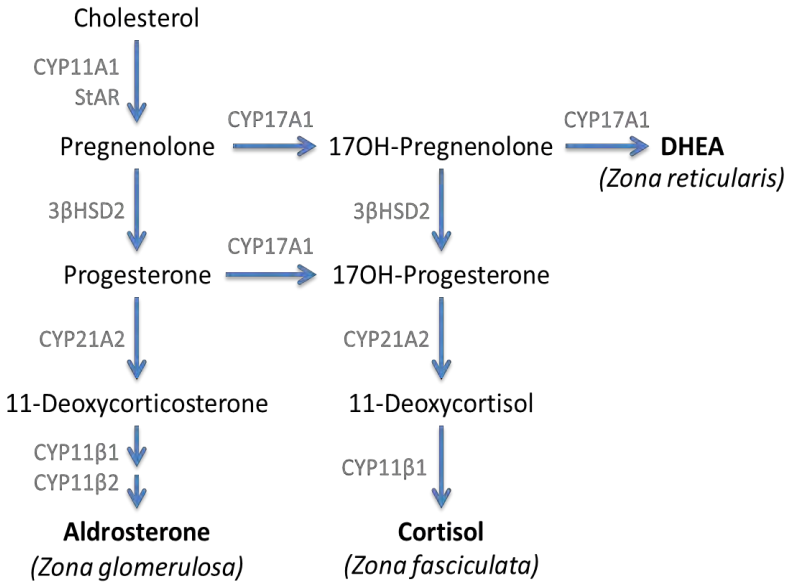

Figure 1: The three major branches of steroidogenesis in humans.

The adrenal cortex is subdivided into three distinct regions, which are capable of metabolising cholesterol into mineralocorticoids, glucocorticoids or sex steroids. In the zona glomerulosa the primary mineralocorticoid aldosterone is produced. Meanwhile, in the zona fasciculata cholesterol is primarily metabolised to generate the glucocorticoid, cortisol. Furthermore, the generation of the primary sex steroid precursor DHEA from cholesterol occurs within the zona reticularis.

1.1.1 Sex steroid synthesis

The biosynthesis of the sex steroids, androgens and oestrogens, is important for development and sexual maturity in both men and premenopausal women, respectively. The enzyme CYP17A1 allows for further downstream conversion of pregnenolone towards the androgen biosynthesis pathway (Miller and Auchus, 2010). CYP17A1 is principally expressed in the adrenal and the gonads (Chung et al., 1987) and has two distinct enzyme activities. Its 17α-hydroxylase activity catalyses pregnenolone to 17α hydroxypregnenolone and its 17,20-lyase activity subsequently coverts 17α hydroxypregnenolone to dehydroepiandrosterone (DHEA) (Nakajin et al., 1984). DHEA is the principal sex steroid precursor, however mostly it is converted to its inactive form dehydroepiandrosterone sulphate (DHEAS) via sulphotransferase enzymes (Auchus, 2004). The enzyme 3β-hydroxysteroid dehydrogenase type 2 (3βHSD2) catalyses the synthesis of androstenedione, while 17β-hydroxysteroid dehydrogenase type five (17βHSD5) is responsible for testosterone synthesis in the *zona reticularis* (Nakamura et al., 2009) (Figure 2).

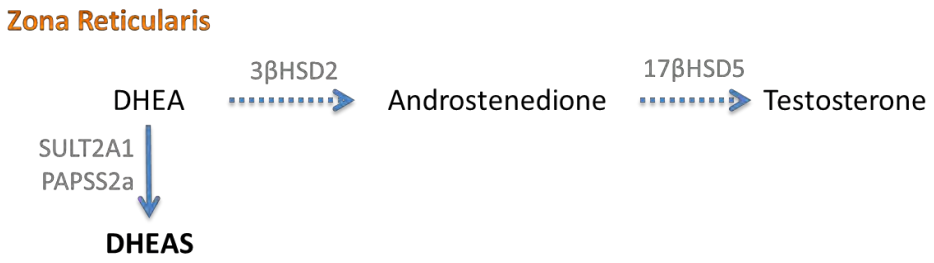

Figure 2: Downstream conversion of DHEA in the zona reticularis

DHEA is produced in the zona reticularis and is primarily sulphonated by DHEA sulphotransferase (SULT2A1) to produce its inactive from, DHEAS. The zona reticularis expresses low levels of 3βHSD2 and 17βHSD5, which allows for only minor conversion of DHEA to androstetenedione and subsequently testosterone. Minor pathways are represented by dashed arrows.

Synthesis of testosterone in men occurs within the testicular Leydig cells where cholesterol is converted to DHEA via a similar pathway to the *zona reticularis* of the adrenal gland. The Leydig cells express both 17βHSD3 and 3βHSD2, but lack the ability to generate DHEAS. Therefore, DHEA produced in the testis is readily converted to testosterone via androstenedione or androstenediol (Miller and Auchus, 2010). Ovarian steroidogenesis occurs in the granulosa and the theca cells which surround the oocyte and form the follicle. Steroidogenesis varies during the menstrual cycle resulting in oestradiol as the major product during the follicular phase and progesterone as the major product produced during the luteal phase (Miller and Auchus, 2010). Thus the regulation of sex steroid synthesis relies on the cell-specific expression of steroidogenic enzymes within the gonads.

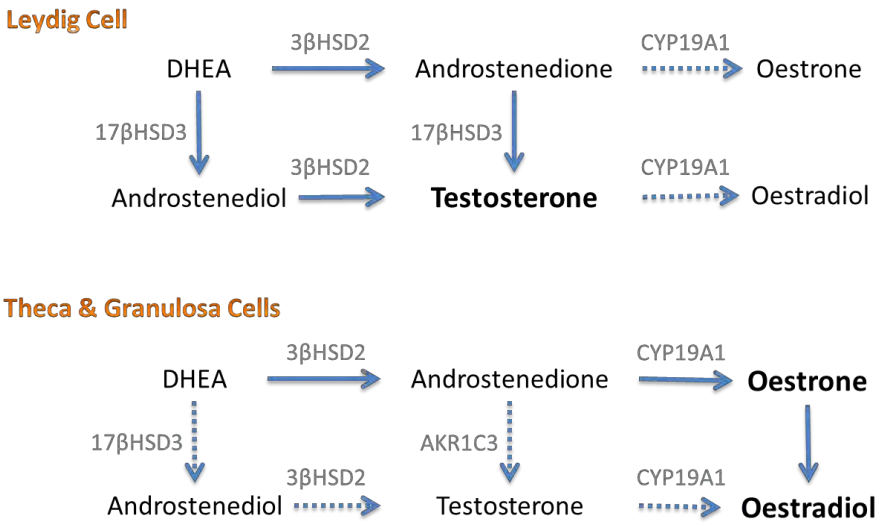

Figure 3: Conversion of DHEA to androgens and oestrogens within the gonads.

The Leydig cells of the testis express high amounts of 17βHSD3 and 3βHSD2, which allows DHEA to be readily converted to testosterone via androstenediol or androstenedione. The ovarian theca and granulosa cells produce the major female sex steroids. Typically, theca cells produce androstenedione which diffuses to the granulosa cells where it is converted to oestradiol or oestrone via CYP19A1 and 17βHSD1. Minor pathways are represented by dashed arrows.

1.2 DHEA and DHEAS

DHEA and its sulphate ester DHEAS are the most abundant circulating steroids in humans (Ebeling and Koivisto, 1994). The major role of DHEA is to act as a precursor for the sex hormones testosterone and oestradiol. During steroidogenesis, DHEA molecules are converted directly to androgens. The sulphate group of DHEAS must first be cleaved to undergo this conversion. Steroid sulphatase is the enzyme responsible for the conversion of DHEAS to DHEA. However, the predominant reaction appears to be the conversion of DHEA to DHEAS via sulphotransferase enzymes, namely DHEA sulphotransferase (SULT2A1) (Hammer et al., 2005). Since sulphonation is a reversible

process, it acts as an on/off switch, and therefore provides another level at which androgen synthesis can be regulated.

Interestingly, the levels of DHEAS varies throughout life following an age-associated pattern. In humans, along with rabbit, dog and chimpanzee have an increase in DHEAS concentration coinciding with sexual maturation (Figure 4) (Cutler et al., 1978). DHEAS concentrations reach their peak level in men aged 20 to 24 years (3470ng/ml) and in women aged 15 to 19 years (2470 ng/ml) which is followed by a steady age-related decline throughout adulthood (Hazeldine et al., 2010, Orentreich et al., 1984).

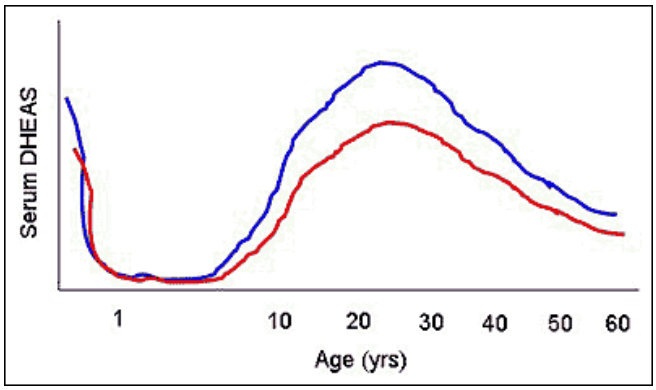

Figure 4: Schematic representation of DHEAS serum levels during life.

Androgen precursors; DHEAS and DHEA have altered concentrations thoughout life. Both in men (blue) and women (red) the levels of DHEAS peak during sexual maturation and then undergo an age related decline often referred to as adrenopause.

1.3 Sulphonation

Sulphonation involves the addition of a sulphate group (SO_3^{-1}) to a molecule and therefore influences its structural and functional characteristics. Sulphate conjugation

plays an important role in the modification of hormones, neurotransmitters, proteins, carbohydrates, lipids, drugs and other xenobiotics (Xu et al., 2002). Sulphonation generally acts as a mechanism of detoxification, as it increases water solubility and therefore aids excretion via the kidneys (Gamage et al., 2006). However, sulphonation of molecules can also cause metabolic activation of pathways or activate molecules to elicit biological effects. In addition, it is believed that the sulphonation of steroid precursors is a mechanism of inactivation, which can be readily reversed when the substrate is required for further steroidogenesis (Gamage et al., 2006). However, it is currently unknown if the sulphonated steroids have specific biological roles or if they are simply inactivated forms of steroids (Miller and Auchus, 2010).

1.4 Sulphotransferases

Sulphonation reactions are catalysed by a super family of enzymes known as sulphotransferases (SULT). There are two broad classes of SULT enzymes. Firstly, the membrane bound SULTs are located in the Golgi apparatus and facilitate the sulphonation of peptides, proteins, lipids, and glycosaminoglycans. The second group of SULTs are located in the cytoplasm and result in the sulphonation of xenobiotics and small endogenous substrates such as steroids, bile acids, and neurotransmitters (Gamage et al., 2006). There are five known classes of SULT enzymes based on amino acid similarity; SULT1, SULT2, SULT3, SULT4 and SULT5 (Blanchard et al., 2004). Additionally, each SULT enzyme has a specific tissue expression pattern and unique substrates.

The SULT1 family has four sub-families (1A, 1B, 1C and 1E). SULT1E1 is one of the most studied SULTs due it is role in steroid homeostasis. This family member has high affinity for oestradiol, oestrone as well as synthetic oestrogens (Falany, 1997). SULT1B1 is expressed in the liver, colon and small intestine and is the major sulphotransferase responsible for sulphonating thyroid hormone (Fujita et al., 1997). SULT1A1 is the dominant sulphotransferase expressed in the human liver and has specificity for phenolic drugs and catecholamines. Other family members such as 1A2, 1C1 and 1C4 have unknown substrates and still require further characterisation (Gamage et al., 2006).

The SULT2 family contains the hydroxysteroid sulphotransferases and consists of two sub-families (2A and 2B). SULT2A1 is commonly referred to as DHEA sulphotransferase as it is the main enzyme responsible for the sulphonation of DHEA. Although DHEA is considered to be its major substrate, SULT2A1 has broad range substrate affinity, including androsterone, pregnenolone, testosterone and oestradiol (Gamage et al., 2006, Strott, 2002). SULT2A1 is highly expressed in the adrenal glands, one of the major sites of DHEA production, and is also expressed in the liver where it is essential for the sulphonation of bile acids and many dietary xenobiotics and drugs (Strott, 2002, Nowell and Falany, 2006). The other member of the SULT2 family is SULT2B1. This enzyme is responsible for the sulphonation of cholesterol, pregnenolone and can also sulphonate DHEA. However in contrast to SULT2A1, SULT2B1 cannot sulphonate androsterone, testosterone, or oestradiol.

Other families of SULTs still remain uncharacterised. Enzymes within the SULT3 family have only been found in mice and rabbits where it specifically sulphonates amino groups. In addition, SULT5A1 has only been reported in mouse DNA databases and therefore this sulphotransferase also remains to be characterised (Falany et al., 2000).

Mutations rendering non-functional SULT proteins in humans have not been described yet; however, single nuclear polymorphisms that result in amino acid changes have been published. The African-American population is known to have a high incidence of polymorphisms in *SULT2A1*, which in turn alters their rate of conversion of DHEA to DHEAS (Thomae et al., 2002). These polymorphisms are associated with an increased risk of prostate and other cancers within this population (Nowell and Falany, 2006). There is continued interest in the role of steroid sulphotransferases in endocrine-dependent cancers such as breast cancer and carcinoma of the prostate gland. As only non-sulphonated steroid hormones can interact with their specific receptors and for example, promote abnormal growth in cancer, the regulation of sulphotransferases may have important pathological implications for these diseases (Strott, 2002).

1.5 PAPS

PAPS or 3´-phosphoadenosine 5´-phosphosulfate acts as the universal sulphate donor for all sulphotransferase reactions (Xu et al., 2000). In mammals, sulphotransferases require a PAPS molecule to donate a SO_3^{-1} group which is transferred to a hydroxyl or amino

group on a suitable acceptor molecule. PAPS is synthesised from ATP by two enzymatic reactions. Firstly, ATP sulphurylase activity enables the generation of adenosine 5´-phosphosulphate (APS) from ATP and sulphate (SO_4). Secondly, APS kinase activity uses a phosphate from an additional ATP molecule to covert APS to PAPS (Strott, 2002). In humans, the enzyme responsible for the generation of PAPS is the bi-functional protein PAPS synthase (PAPSS) (Figure 5).

1.6 PAPS Synthase

In prokaryotes, PAPS is synthesised by two distinct enzymes, ATP sulphurylase and APS kinase (Klaassen and Boles, 1997). However, in higher organisms PAPS synthase enzymes contain both functional domains and therefore are capable of catalysing both reactions sequentially (Figure 5). It is believed that the fusion of the two proteins increases catalytic efficiency by a channelling mechanism for APS between the two PAPSS active sites (Lyle et al., 1994). In humans, there are two isoforms of PAPS synthases, which are 77% identical at the protein level (Strott, 2002). These two isoforms, PAPSS1 and PAPSS2, are encoded on separate chromosomes and differ in their expression patterns, cellular localisation and levels of catalytic activity.

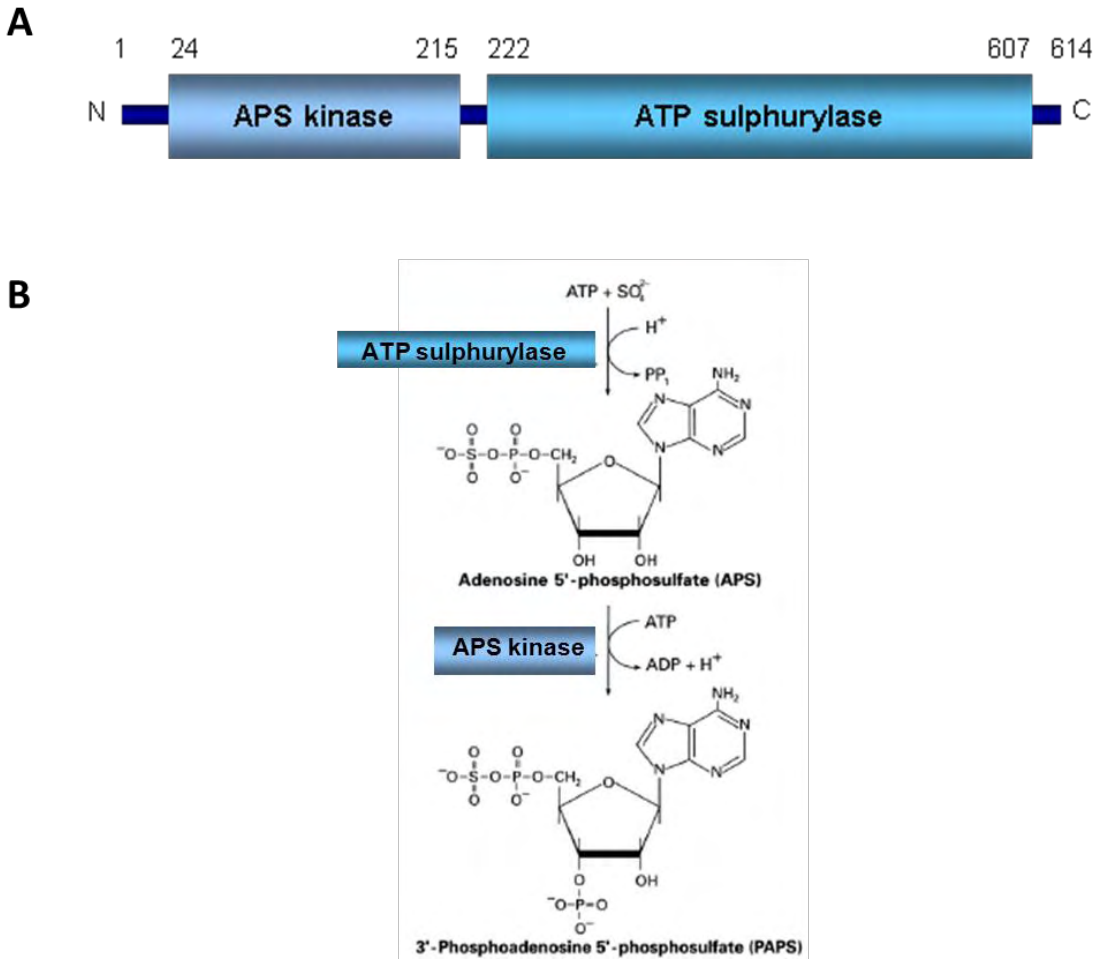

Figure 5: Schematic depiction of hsPAPSS2a protein structure and function.

(A) PAPSS2a consists of two major protein domains; the carboxyl ATP sulphurylase domain and the amino terminal APS kinase domain synthesises. (B) Initially, the ATP sulphurylase domain generates adenosine 5´-phosphosulphate APS from ATP and sulphate. Secondly, the APS kinase domain synthesises PAPS by phosphorlylating APS. Adapted from (Strott, 2002).

In humans, *PAPSS1* is located on chromosome four and is ubiquitously expressed (Xu et al., 2000). To date, functionally disrupting mutations in *PAPSS1* have been described in humans. It has been suggested that due to its ubiquitous expression, non-functional

mutations could be embryonic lethal (Miller and Auchus, 2010). Although it is believed that PAPS synthesis occurs in the cytosol, PAPSS1 localises to the nucleus through a 21 amino acid segment at the amino terminus (Besset et al., 2000). Furthermore, PAPSS2, which typically localises to the cytoplasm is capable of translocating to the nucleus in the presence of PAPSS1 (Besset et al., 2000). The precise implications of the specific subcellular localisation of the PAPS synthase isoforms is yet to be fully understood.

Human *PAPSS2* is located on chromosome 10 (Faiyaz ul Haque et al., 1998). In both mice and humans, *PAPSS2* undergoes alternative splicing (Kurima et al., 1999), resulting in two variants, *PAPSS2a* and *PAPSS2b*, that differ in the presence or absence of five amino acids within the ATP sulphurylase domain (Strott, 2002). PAPSS2 is highly expressed in cartilage, adrenal tissues and the liver (Fuda et al., 2002). Unlike PAPSS1, several functional disrupting mutations within *PAPSS2* have been identified in mouse and humans. These are associated with a brachymorphic phenotype in mouse (Faiyaz ul Haque et al., 1998), bone growth defects in humans (Faiyaz ul Haque et al., 1998, Ahmad et al., 1998) and disrupted steroid metabolism resulting in androgen excess in women (Noordam et al., 2009). PAPSS1 and PAPSS2 are capable of forming homodimers and heterodimers (Grum et al., 2010). The significance of this interaction is unknown, but it hypothesised to influence the cellular localisation of the PAPS synthase isoforms and therefore regulate their activity. Currently, the importance of having two PAPS synthase proteins which perform identical functions is unknown. It has been suggested that each PAPS synthase enzyme may have specific physiological roles which are regulated by their cellular localisation and their ability to form heterodimers (Grum et al., 2010).

1.7 PAPSS2 Genetic Variants

Reported mutations within the *PAPSS2* gene are linked to an increasing number of human diseases. Complete loss of PAPSS2 function was found to be the cause of spondyloepimetaphyseal dysplasia of the Pakistani type in one family cohort. Members of this family were found to carry a nonsense mutation at serine 475 of PAPSS2 (S475X). They presented with short stature, short bowed lower limbs, mild brachydactyly (shortness of the fingers and toes), kyphoscoliosis (abnormal curvature of the spine), an abnormal gait, enlarged knee joints and osteoarthritis (Ahmad et al, 1998), implying an important role for PAPSS2 in cartilage and bone formation.

Mutations within PAPSS2 have also been associated with an excess androgen phenotype. In 2009, PAPSS2 deficiency was discovered in a patient with premature pubarche (Noordam et al, 2009). At the age of six this female patient presented with premature pubarche and advanced bone age. At the age of 13 she presented with worsening of androgen excess associated with acne, hirsutism and secondary amenorrhea. It was observed that her circulating DHEA, androstenedione, testosterone and dihydrotesterone were all significantly elevated, whereas her DHEAS levels were undetectable. The patient was found to have a maternally inherited PAPSS2 nonsense mutation at arginine 329 (R329X). In addition, the patient also carried a paternally inherited PAPSS2 missense mutation changing a tyrosine to an arginine at amino acid position 48 (T48R). *In vitro* functional characterisation of both mutations revealed that R329X had no activity, while the T48R mutation had approximately 6% residual activity when compared to PAPSS2 wild type protein (Noordam et al., 2009). The deficiency in

PAPSS2 in this patient prevented the sulphonation of DHEA and consequently caused an excess production of androgens.

Xu and colleagues (2002) have additionally identified four coding region single nucleotide polymorphisms (SNPs), which cause amino acid sequence changes (E10K, M281L, V291M, R432K). Functional characterisation of these PAPSS2 variants was carried out in a two-step process. Initially, PAPS was generated from ATP and Na_2SO_4 in COS-1 cells expressing recombinant his-tagged hsPAPSS2 variants. Subsequently, an aliquot from this PAPS generating step was used as a substrate for the sulphonation of radioactive oestradiol catalysed by recombinant human SULT1E1 in COS-1 cells. Extraction and measurement of the sulphonated and the non-sulphonated radioactive steroid determined the activity of the hsPAPSS2 variants. Both E10K and V291M had a significant decrease in catalytic activity of 72.6% and 37.1%, respectively (Xu et al., 2002) (Table 1). Additionally, it was shown that E10K was decreased at protein level as determined by western blot.

In human diseases caused by PAPSS2 deficiency, PAPSS1 is unable to compensate for the role of PAPSS2. Specifically, it remains unclear as to how a loss of PAPSS2 function results in an osteochondrodysplasia phenotype despite abundant expression of PAPSS1 in cartilaginous tissue (Faiyaz ul Haque et al., 1998). Additionally, several variants of human PAPSS2 have been described to be associated with changes in functional activity resulting in clinical phenotypes. Two variants are associated with hyperandrogenism (Noordam et al., 2009), while another results in a severe bone phenotype (Faiyaz ul

Haque et al., 1998). It has been suggested that PAPSS2 activity impacts independently on differing sulphation processes resulting in specific clinical symptoms. It is hypothesised that genetic variants of PAPSS2 have varying abilities to generate PAPS and therefore altered abilities to sulphonate molecules through specific sulphotransferases.

PAPSS2A variant	Activity (%WT)		Frequency
	SULT2A1	SULT1E1	
E10K	-	73	0.006
T48R	6	-	<0.005
M281L	-	100	0.006
V291M	-	37	0.017
E332G			
R329X	0	-	<0.005
D370G			
R432K	-	100	<0.005
A463V			
S475X	0	-	<0.005

Table 1: Functional activity and population frequency of PAPSS2a genetic variants

To date there have been ten PAPSS2a genetic variants reported in humans. PAPSS2a T48R, R329X and S475X were reported to have 6%, 0% and 0%, respectively within the DHEA sulphonation pathway. Additionally, PAPSS2a E10K, M281L, V291M, and R432K showed 73%, 100%, 37% and 100% activity respectively, in sulphonation of oestrogen. PAPSS2a E332G, D370G and A463V remain uncharacterised. PAPSS2a V291M is the only variant to have a population frequency greater than 0.01%.

2 PROJECT AIMS

This project aims to characterise the functional impact of hsPAPSS2a mutants on the DHEA sulphation pathway. The following objectives will be addressed;

- To determine the functional ability of the previously uncharacterised hsPAPSS2a E332K genetic variant in its ability to generate PAPS for DHEA sulphonation via SULT2A1.
- To determine the functional ability of hsPAPSS2a E10K and M281L genetic variants in their ability to generate PAPS for DHEA sulphonation via SULT2A1. These genetic variants have previously been characterised in oestrogen sulphonation, however, characterisation of these variants in sulphonating DHEA will establish if genetic variants have differing functional capacities for different sulphonation pathways.
- The generation of stable cell lines expressing hsPAPSS2a and hsSULT2A1 to allow for characterisation of PAPSS2a genetic variants *in vitro.*

3 MATERIALS AND METHODS

3.1 Molecular Biology

3.1.1 Transformation of E. Coli by Heat Shock

Transformation is a naturally occurring process that allows the uptake of circular plasmid DNA by bacteria. Molecular biology techniques can manipulate this process by allowing competent bacteria to uptake plasmids containing genes of interest. As the bacteria replicate they make copies of the recombinant plasmid, which can be purified for future work.

Bronze Efficiency Competent DH5α *E. coli* cells (Bioline) were transformed by incubating with a recombinant plasmid and using a heat shock method. Typically, 1μL of DNA was added to 40μL of competent cells. The mixture was placed on ice for 20 minutes before heat shocking at 37°C for one minute and then returned to ice for five minutes. 200μL of Luria Bertani (LB) media (Sigma) was added to the cells and incubated for 20 minutes at 37°C. Finally, the cell suspension was plated onto LB agar plates containing Carbenicillin (Sigma) at 50μg/mL for selection. The agar plates were incubated at 37°C for 16 hours.

3.1.2 Plasmid DNA preparation

Plasmid DNA preparation is a method which enables the extraction and purification of

plasmid DNA from bacteria. Plasmids were prepared using the QIAprep Spin Miniprep kit as per the manufacturer's instructions (Qiagen). This kit uses an alkaline lysis method of bacterial cells and allows the plasmids to bind onto silica containing high salt. Typically, a single *E. coli* colony was used to inoculate 10mL of LB media containing 50µg/mL carbenicillin. They were cultured at 37°C for 16 hours with shaking/aeration at 250rpm. The culture was centrifuged at 3,000rpm for five minutes to pellet the bacteria. The cells were then resuspended in 250µL P1 buffer (50mM Tris-Cl, pH 8.0; 10mM EDTA; 100 µg/mL RNase A). The bacteria were lysed using 250µL P2 buffer (200 mM NaOH, 1 % SDS [w/v]) and neutralised by adding 350µL acetate containing N3 buffer. Samples were then centrifuged for 10 minutes at 13,000rpm. The remaining supernatant was added to the QIAprep Spin Column and centrifuged for one minute to allow plasmid DNA to bind to the column. The column was washed by adding 750µL of ethanol containing PE buffer and centrifuged for one minute. The column was then centrifuged for an additional minute to remove residual wash buffer. Finally, the purified plasmid DNA was eluted by adding 40µL of deionised water to the column and centrifuged for one minute. Plasmid concentration and purity was determined (section 3.1.3) and samples were stored at -20°C.

3.1.3 Quantification of Nucleic Acids

Purified plasmids and extracted RNA were all quantified using the NanoDrop® ND-1000 spectrophotometer. Typically, distilled water was used to determine a background level and then 1.5µL of sample was applied onto the spectrophotometer. For nucleic acid

samples a ratio of A260/A280 was used to determine purity. A ratio between 1.8 and 2.2 was usually considered acceptable to use in future experiments.

3.1.4 Site Directed Mutagenesis

Site direct mutagenesis is a PCR based approach that uses specifically designed oligonucleotides containing mismatched base pairs to obtain the desired mutation. Initially, forward and reverse oligonucleotides were designed containing specific mutations within the hsPAPSS2 cDNA to generate R432K, E332G, D370G and A463V amino acid mutations (Table 2). Oligonucleotides were synthesised by Sigma.

Oligonucleotide	Sequence (5' - 3')
R432K FORWARD	GCAGGCTCCTAGAGAAGGGCTACAAG
R432K REVERSE	CTTGTAGCCCTTCTCTAGGAGCCTGC
E332G FORWARD	GGGTAGCTATCTTACGAGACGCTGGATTCTATGA
E332G REVERSE	TCATAGAATCCAGCGTCTCGTAAGATAGCTACCC
D370G FORWARD	CTGGTTGGTGGAGGCCTTCAGGTGCTG
D370G REVERSE	CAGCACCTGAAGGCCTCCACCAACCAG
A463V FORWARD	TGAAGCACGTGGCTGTGCTCGA
A463V REVERSE	TCGAGCACAGCCACGTGCTGCTTCA

Table 2: Site Directed Mutagenesis Oligonucleotides

Forward and reverse oligonucleotide primers were designed to introduce amino acid cDNA changes to generate PAPSS2a R432K, E332G, D370G and A463V. Mismatched nucleotides are underlined.

Subsequent site directed mutagenesis was performed using the QuickChange® II XL site-directed mutagenesis kit (Stratagene) (Figure 6). Firstly, this kit uses PCR to induce the mutation using specifically designed oligonucleotides containing the required mutation. The site directed mutagenesis reaction was carried out in 50µL reaction volumes containing 1X reaction buffer, 10ng of template plasmid DNA, 1µL of dNTP mix, 3µL of Quick Solution reagent, 2.5U *PfuUltra* HF DNA polymerase, 125ng of forward mutagenesis oligonucleotide and 125ng of reverse mutagenesis oligonucleotide. Cycling condition included 95ºC for one minute followed by 18 cycles of denaturing at 95ºC for 50 seconds, annealing at 60ºC for 50 seconds and extension at 68ºC for 15 minutes. A final extension at 68ºC for four minutes was used to complete the cycling conditions. Following the PCR amplification the reaction was treated with 1µL of *DpnI* restriction enzyme and incubated at 37ºC for one hour to digest methylated template DNA. Finally, the mutated plasmid was transformed into ultra-competent XL1-Blue *E. coli* cells (section 3.1.1). Individual clones were screened via DNA sequencing (section 3.1.5).

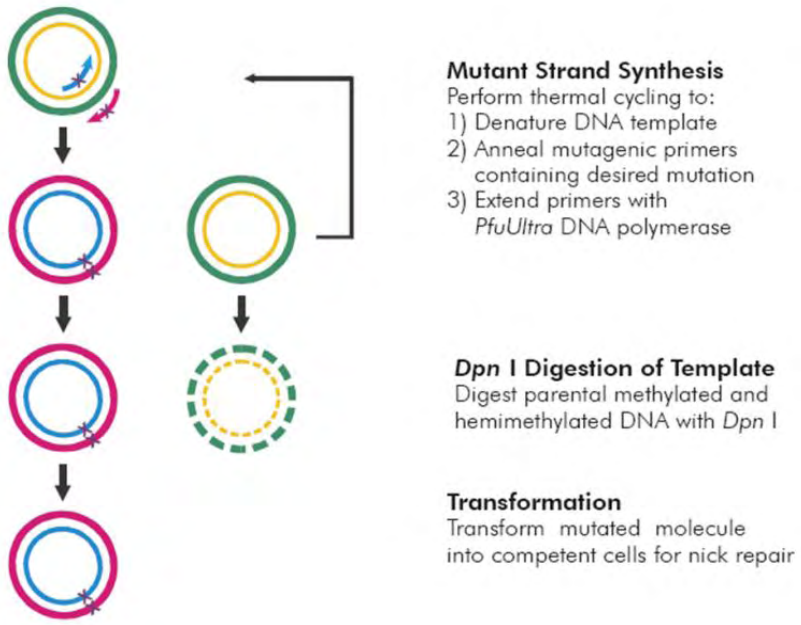

Figure 6: Site Direct Mutagenesis methodology

For each PAPSS2a genetic variant, forward and reverse oligonucleotides were designed containing a single mismatched nucleotide to engineer the desired amino acid change. Denaturing of the plasmid DNA template (yellow and green) allowed the oligonucleotides to bind to the template. Subsequently, plasmids were amplified by DNA polymerase allowing of incorporation of mismatched base. Treatment with DpnI caused digestion of methylated parental bacterial DNA. Therefore it will remove the template plasmid DNA and leave only the PCR amplified mutated plasmids.

3.1.5 DNA sequencing

DNA sequencing was performed by the Sequencing Facility at the Biosciences School within the University of Birmingham, United Kingdom. Typically, 6.4pmol of sequence primer and 400-1000ng of double stranded plasmid DNA was supplied in 10µL of deionised water. Assembled sequence data was viewed and analysed by SeqMan Pro software (Laser Gene).

3.1.6 RNA extraction

RNA extraction is a procedure which allows for the isolation of RNA from a biological sample and therefore gives a snapshot of the genes being actively transcribed at that time point. RNA was isolated from transfected HEK293 cells using TRI Reagent (Sigma). Typically, cells were washed twice in phosphate buffered saline (PBS) (Sigma) before 1mL of TRI Reagent was added. Cells were harvested using a cell scraper and the suspension was placed in a 1.5mL microcentrifuge tube. 200µL of chloroform was then added to the samples and they were mixed vigorously. Samples were incubated at room temperature for 10 minutes and centrifuged at 13,000rpm for 20 minutes at 4ºC. The upper aqueous phase containing the RNA was transferred to a fresh 1.5mL tube. The RNA was precipitated using 500µL of cold isopropyl alcohol. Samples were incubated for at least 20 minutes at -20ºC. The RNA was pelleted by centrifugation at 13,000rpm for 10 minutes at 4ºC and washed in 70% ethanol, followed by a further centrifugation step at 13,000rpm from 10 minutes at 4ºC. RNA was resuspended in RNase-free water, quantified (section 3.1.3) and stored at -20ºC.

3.1.7 Reverse Transcription

Reverse transcription (RT) is a methodology that allows for the generation of complementary DNA (cDNA) from a purified RNA sample. cDNA was prepared from total RNA using TaqMan Reverse Transcriptase kit according to the manufactures instructions (Applied Biosystems). Typically 20µL reactions were made containing; 1X reaction buffer, 5.5mM magnesium chloride, 500µM of each dNTP, 2.5µM of random

hexamer primers, 0.4U/µL of RNase inhibitor, 1.25U/µL Multiscribe Reverse Transcriptase and 700ng of RNA. Samples were subjected to 25ºC for 10 minutes, 37ºC for one hour, 48ºC for 30 minutes and 95ºC for five minutes in a thermal cycler. cDNA samples were stored at -20ºC until required.

3.1.8 Quantitative Real Time RT PCR

Real time Reverse Transcriptase Polymerase Chain Reaction (RT-PCR) is a method which allows for amplification and simultaneous quantification of specific genes of interest. A fluorescent reporter probe method was used where probes where tagged with the FAM reporter and with a TAMRA quencher.

Typically, 10µL reactions were made consisting of 0.5µL of Assay on Demand (Applied Biosystems) for either hsPAPSS1, hsPAPSS2 or SULT2A1, 5µL of TaqMan Master Mix (Applied Biosystems) and 4.5µL of previously prepared cDNA (section 3.1.7). 18S expression was also analysed by preparing 0.05µL each of 18S forward and reverse primer (Applied Biosystems), 0.05µL of Ribosomal VIC probe (Applied Biosystems), 0.35µL of deionised water, 5µL of TaqMan Master Mix (Applied Biosystems) and 4.5µL of previously prepared cDNA.

Samples were prepared in 96-well optical reaction plates (Applied Biosystems) and sealed with adhesive PCR film (Thermo scientific). Reactions were run on an ABI Prism SDS 7500 Thermocycler for 50°C for two minutes, 95°C for 10 minutes, followed by 40

cycles of 95°C for 15 seconds and 60°C for one minute. Samples were analysed using 7500 System SDS software (Applied Biosystems).

3.2 Cellular Biology

3.2.1 Mammalian Cell Culture

HEK293 cells were cultured in high glucose Dulbecco's Modified Eagle's medium (DMEM) with L-glutamine. Complete media was supplemented with 10% foetal bovine serum (Sigma) and 1% penicillin (5U/mL) streptomycin (5µg/mL) (Invitrogen). Cells were maintained at 5% CO_2 at 37°C in a humidified incubator. HEK293s were cultured on cellBIND flasks (Corning Life Sciences) and were harvested either by trypsin digestion or by using a cell scraper.

3.2.2 Transfection of Mammalian Cell Lines using FuGENE-HD

Transfection is a process which allows introduction of nucleic acids into cells. For transient transfections, FuGENE-HD transfection reagent (Roche) was used. FuGENE-HD contains a blend of cationic lipids which bind to the negatively charged DNA and allows it to be taken up by the cell. The day before transfection HEK293 cells were seeded at $20x10^4$ cells per well of a six-well cellBIND plate (Corning Life Sciences).

Typically, 2µg of purified plasmid DNA was mixed with 8µL of Fugene reagent in 100µL of serum free high glucose DMEM. This was incubated at room temperature for

15 minutes to allow the FuGENE and DNA to form complexes. The HEK293 cells received 2mL of fresh culture medium before 100µL of DNA-FuGENE mix was added to the cells. The cells were then incubated at 37°C, 5% CO_2 for 48 hours prior to sulphonation assays (section 3.3.1).

3.2.3 Transfection of Mammalian Cell Lines using Lipofectamine-2000

The day before transfections HEK293 cells were seeded at $20x10^4$ cells per well of a six well cellBIND plate (Corning Life Science). For transfections, 4µg of plasmid DNA and 10µL of Lipofectamine 2000 reagent (Invitrogen) were diluted separately in 50µL of Opti-MEM Media (Gibco) and incubated at room temperature for five minutes. The plasmid and Lipofectamine 2000 mix were combined and incubated for a further 20 minutes at room temperature. Cells received 2mL of fresh culture media before 100µL of DNA-lipofectamine mix was added to the cells. The cells were then incubated at 37°C, 5% CO_2 for 48 hours. Media was replaced after 48 hours and supplemented with 500µg/mL geneticin antibiotic to select cells expressing the plasmid DNA.

3.2.4 Protein extraction

HEK293 cells were washed twice in PBS before being harvested in 1mL of PBS using a cell scraper. To extract protein, 500µL of SDS loading buffer was added (50mM Tris-HCl pH6.8, 10% glycerol, 2% SDS, 1% β-mercaptoethanol, 0.05% bromophenol blue) Samples were then heated to 95ºC on a heat block for 10 minutes. This caused the cells to burst releasing the protein and allowing the SDS to bind. Protein samples were stored at

-20ºC and care was taken to limit the number of freeze thaw cycles.

3.2.5 SDS Poly Acrylamide Gel Electrophoresis

Sodium dodecyl sulfate polyacrylamide gel electrophoresis or SDS PAGE is a technique that allows for the separation of proteins based on size. Typically, 10-30µL of protein sample was loaded on a 10% NuPAGE Novex Tris-Bis precast gel (Invitrogen) and run at 200 volts for one hour in 1X NuPAGE Buffer (Invitrogen). Upon completion of electrophoresis the gels were transferred to nitrocellulose membranes.

For the protein transfer, blotting pads, absorbent Whatman filter papers and the nitrocellulose membrane (GE Healthcare) were equilibrated in 1X transfer buffer (25mM Tris, 190mM glycine and 20% (v/v) methanol) (National Diagnostics). The transfer apparatus was assembled and run at 30 volts for one hour. After the transfer was complete Ponceau S staining (Sigma) was used to confirm successful transfer of the proteins from the polyacrylamide gel to the nitrocellulose membrane. The membrane was simply placed in the stain until protein bands were visible. The membrane was washed several times before proceeding with western blotting (section 3.2.6).

3.2.6 Western Blot

Western Blot is an analytical technique that uses specific antibodies to detect proteins of interest which have previously been separated based on their size. Primary antibodies used for western blotting analysis included rabbit-anti-hsPAPSS2 (abcam ab37611) used

in a 1:1000 dilution and mouse-anti-hsβ-actin-HRP (abcam ab20272) used in a 1:20,000 dilution. Secondary antibody detection used the goat-anit-rabbit-HRP (Dako PO448) in a 1:1000 dilution.

Initially, the membrane was blocked for one hour using blocking buffer (10% skim milk in PBS). The membrane was incubated overnight at 4ºC with primary antibody at the required dilution in blocking buffer. The following day the membrane was washed three times for five minutes in PBS with 0.1% Tween 20 (PBST). The secondary antibody was diluted to the appropriate concentration in blocking buffer and incubated with the membrane for one hour. Finally the membrane was washed three times for five minutes in PBST. Following antibody incubation, the blot was developed using ECL detection kit (GE health care) according to the manufactures instructions and Kodak film.

3.3 Biochemical Analysis

3.3.1 DHEA to DHEAS Sulphonation Assay

The enzymatic activity of hsPAPSS2a genetic variants was measured by the ability of HEK293 cells to convert tritiated (3H) DHEA to DHEAS. HEK293 cells were transfected with purified bicistronic pIRES plasmid containing the hsPAPSS2A variant and hsSULT2A1 48 hours prior to assay (section 3.2.2). 48 hours after transfection the cells were incubated at 37ºC for two hours with 500µL of serum-free high glucose DMEM containing 0.2µCi 3H-DHEA and 125nM of unlabelled DHEA. Each assay was performed in triplicate and repeated a minimum of three times to determine accurate

values. After incubation with the steroids extraction of DHEA and DHEAS was performed for each sample (section 3.3.2).

3.3.2 Extraction of DHEA and DHEAS

In order to determine the functional ability of PAPSS2a and SULT2A1 to covert DHEA to DHEAS, all the DHEA and DHEAS were extracted from the cell culture media before analysis. After the assay, media from each sample was collected in individual glass test tubes and 5mL of dichloromethane was used to extract the steroids. In addition, 1mL of 100% methanol was added to individual wells in order to extract residual steroids. These fractions were also collected in individual glass test tubes and allowed to evaporate. Dichloromethane factions were vortexed thoroughly and centrifuged at 1,500rpm for five minutes to ensure separation of the top aqueous phase and lower organic solvent phase. The top phases were aspirated off and the remaining fraction containing the extracted steroid was added to the corresponding methanol fraction. These were then allowed to evaporate on a sample concentrator at 50ºC. The extracted steroids were then prepared for chromatography analysis (section 3.3.3).

3.3.3 Thin Layer Chromatography

Thin layer chromatography (TLC) is a technique that allows the separation of mixture up a plate coated with a thin layer of cellulose, aluminium oxide, or silica. Once the sample has been applied to the plate, a mixture of solvents is drawn up the plate via capillary action. Molecules will travel at different rates up the TLC plate allowing for separation.

After the extraction of DHEA and DHEAS from the cell media, the steroids were resuspended in 70µL of dichloromethane. The steroids were spotted onto PE SIL G/UV silica gel TLC plates and separated in a solvent system consisting of eight parts chloroform, two parts acetone, four parts acetic acid, two parts methanol and one part water. Plates were allowed to run for 90 minutes to ensure adequate separation of DHEA and DHEAS fractions. Plates were then removed from the tank and allowed to air dry. Purified samples of 3H-DHEA and 3H-DHEAS were also spotted on the plates as a standard control.

Radioactivity was detected directly from the TLC plate by the AR2000 imaging scanner and analysed using the Laura radio-chromatography system software (Lab Logic). Radioactivity was detected for five minutes per sample.

4 RESULTS

4.1 Site Directed Mutagenesis

Site direct mutagenesis was used to introduce specific changes to *hsPAPSS2a* cDNA so that naturally occurring genetic variants could be characterised *in vitro.* The bicistronic pIRES vector was used as it is a mammalian expression system which allows simultaneous expression of *hsPAPSS2a* and *hsSULT2A1* from a single mRNA transcript. Constructs containing cDNA for *hsPAPSS2a* wild type or genetic variant (E10K, M281L, V291M, T48R, R3S9X and S475X) cloned into the first multiple cloning site and *hsSULT2A1* cDNA in the second were already available (Vivek Dhir) (Figure 7).

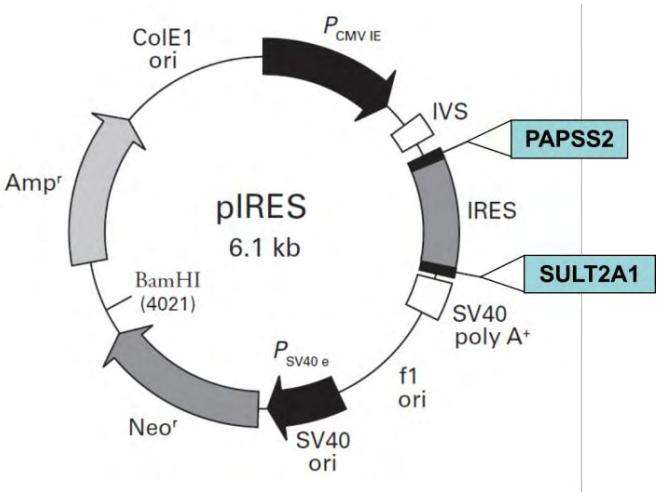

Figure 7: pIRES:yhsPAPSS2a/hsSULT2A1 expression plasmid.

The bicistornic pIRES plasmid was used to express the hsPAPSS2a genetic variants and hsSULT2a. For all constructs hsPAPSS2a was cloned into the first multiple cloning site while hsSULT2A1 was cloned into the second. This plasmid allows expression of both hsPAPSS2a and hsSULT2A1 from the same messenger RNA through the internal ribosome entry site (IRES).

pIRES:hsPAPSS2a wild type/hsSULT2A1 was used as a template for all subsequent site direct mutagenesis. Oligonucleotides were designed incorporating specific nucleotide mismatches to induce mutations into the cloned *PAPSS2a* cDNA (section 3.1.4). These mutations, A995G, T1109C, G1295A and C1388T resulted in, E332G, D370G, R432K and A463V amino acid changes, respectively. After site direct mutagenesis was performed, individual clones were confirmed by sequencing the entire *PAPSS2a* cDNA (Figure 8). The sequencing results confirmed the presence of the specific DNA mutations. Alignment of the entire cloned cDNA to *hsPAPSS2a* cDNA reference sequence (GI:62912490) established no other nucleotide changes occurred during amplification. Subsequently, the confirmed hsPAPASS2a variants were subject to functional analysis.

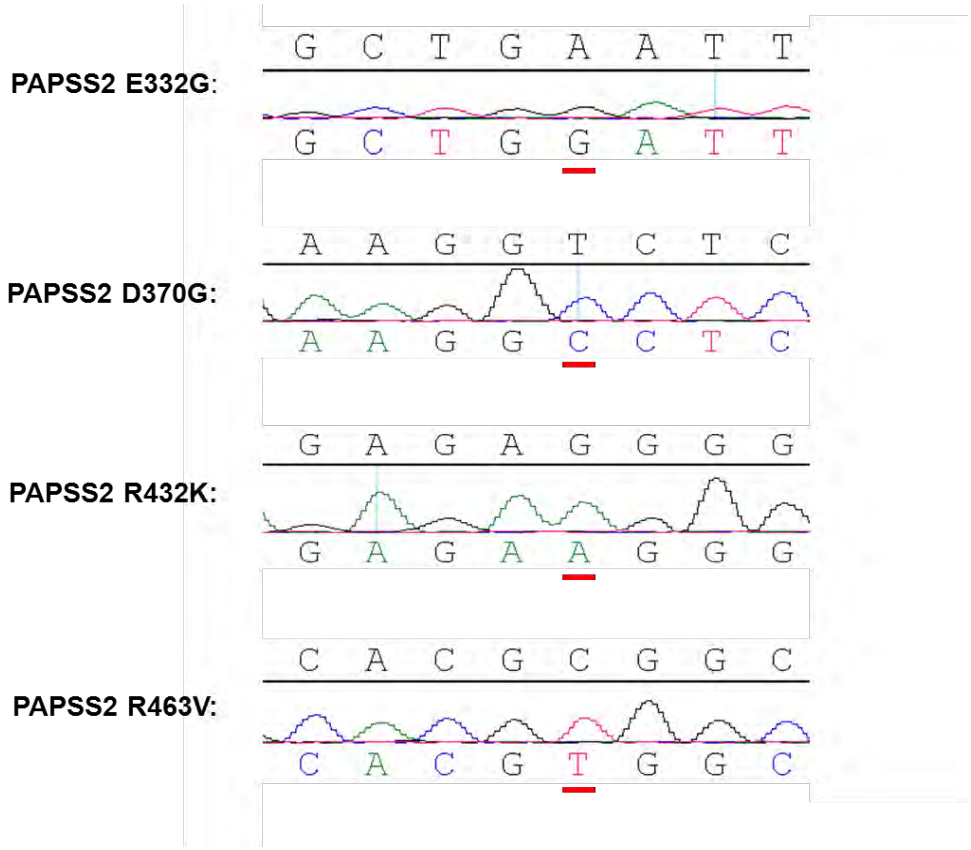

Figure 8: Confirmation of site directed mutagenesis.

Sequencing traces confirm the presence of the desired mutations (underlined) when compared to the PAPSS2a wild type sequence (shown above). The A995G, T1109C, G1295A and C1388T DNA variations result in E332G, D370G, R432K and A463V amino acid changes, respectively. These PAPSS2a genetic variants had not been previously generated within the laboratory.

4.2 *In vitro* analysis of hsPAPSS2a genetic variants

4.2.1 mRNA expression analysis of pIRES:hsPAPSS2/hsSULT2A

In order to functionally characterise hsPAPSS2a genetic variants *in vitro*, each were over expressed in HEK293 cells (section 3.2.2). Quantitative real time RT PCR was used to determine if the level of expression between control cDNAs and the hsPAPSS2a genetic

variants was similar. RNA was extracted from transfected cells overexpressing the pIRES:hsPAPSS2a/hsSULT2A1 constructs and used to generate cDNA (sections 3.1.6 and 3.1.7). Quantitative real time RT PCR was used to determine expression levels of *hsPAPSS1*, *hsPAPSS2a* and *hsSULT2A1* and these were normalised against 18S ribosomal RNA (section 3.1.8). Analysis of mRNA levels showed that typically the genetic variants (E10K, E332G or M281L) had similar levels of expression as the wild type construct within individual experiments (Table 3).

		Gene of Interest expression (delta ct)		
Experiment	**Transfection**	**PAPSS2a**	**SULT2A**	**PAPSS1**
E10K	**PAPSS2a wild type/ SULT2A1**	9.2	9.5	22.2
	PAPSS2a E10K/ SULT2A1	7.5	7.4	21.8
	SULT2A alone	16.2	4.6	23.8
M281L	**PAPSS2a wild type/ SULT2A1**	5.0	5.2	21.3
	PAPSS2a M281L/ SULT2A1	3.6	3.6	22.1
	SULT2A alone	17.2	4.7	21.9
E332G	**PAPSS2a wild type/ SULT2A1**	5.0	5.2	21.3
	PAPSS2a E332G/ SULT2A1	4.3	4.4	21.1
	SULT2A alone	17.2	4.7	21.9

Table 3: Representative expression of PAPSS2a, SULT2A1 and PAPSS1

Analysis of delta ct values were used to determine expression levels of pIRES:hsPAPSS2a/hsSULT2a plasmids within experiments. SULT2A1 showed similar levels of expression for cells transfected with PAPSS2a wild type, the genetic variant or for the SULT2a alone within individual experiments. Differences in transfection efficiency between experiments was observed as PAPSS2a wild type relative expression levels showed delta cts of 9.2 and 5.0.

4.2.2 Functional activity

To determine *in vitro* function of the hsPAPSS2a genetic variants (E10K, M281L and E332G), cells overexpressing pIRES:hsPAPSS2a/hsSULT2A1 plasmids were assayed in optimal hsPAPSS2a wild type conditions (sections 3.2.2 and 3.3.1). A physiological DHEA concentration close to the K*m* of hsPAPSS2a was used and the assays were stopped when DHEA conversion was within the linear phase to ensure accurate conversion rates could be established. Furthermore, HEK293 cells were used for functional analysis because of their inability to endogenously produce DHEA or carry out its sulphonation. The capacity of the hsPAPSS2a variants to generate PAPS was determined by the ability of the co-expressed SULT2A1 to convert 3H-DHEA to 3H-DHEAS.

For each replicate, radiation counts corresponding to 3H-DHEA and 3H-DHEAS peaks were used to determine the percentage of sulphonation that occurred (Figure 9). The average of each experiment was recorded and this was repeated a minimum of three separate occasions. The average conversion rate of wild type hsPAPSS2a assay was assumed to be 100% and this was used to determine the percentage of functional activity for each of the hsPAPSS2a variants. In addition, HEK293 cells express low levels of PAPSS2a. As a control, the activity of HEK293 cells to generate DHEAS in the presence of a sulphotransferase enzyme was determined by overexpressing pIRES:hsSULT2A1. Functional activity of cells transfected with pIRES:hsSULT2A1 was subtracted from all pIRES:hsPAPSS2a/hsSULT2A1 activities to give a representation of the level of sulphonation caused only by the overexpressed cDNAs.

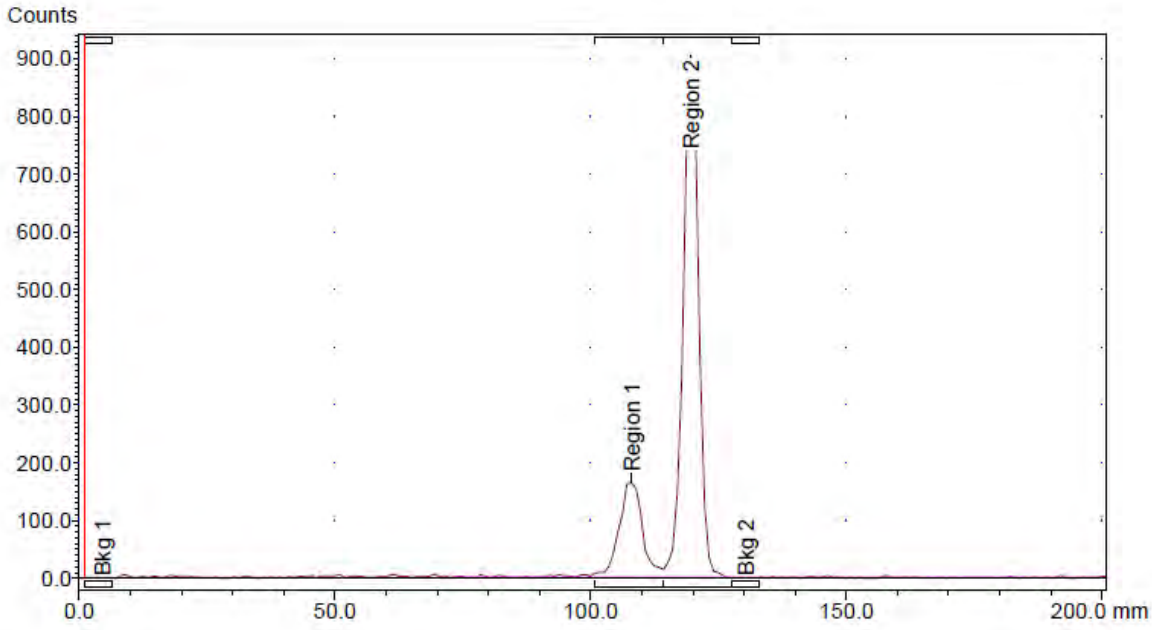

Regions: TLC Detector: AR-2000

Name	Start (mm)	End (mm)	Retention (RF)	Height (Counts)	Area (Counts)	%ROI (%)	%Total (%)
Bkg 1	0.9	6.2	0.017	2.0			
Region 1	100.9	114.2	0.522	165.0	971.6	21.47	21.23
Region 2	114.2	127.6	0.578	906.0	3552.7	78.53	77.62
Bkg 2	127.6	133.0	0.631	3.0			
2 Peaks					4524.3	100.00	98.85

Total Area: 4576.8 Counts
Average Background: 1.6 Counts
Unallocated Area: -360.6 Counts

Method: Prog assays

Run length: 5m1s

Figure 9: Representative TLC plate read out.

Region one corresponds to the extracted 3H-DHEAS while region two represents the extracted 3H-DHEA. From this readout it can be confirmed that the conversion of DHEA to DHEAS was 21.47% for this particular PAPSS2 wildtype assay.

The previously uncharacterised E332G hsPAPSS2a variant showed a significant decrease to 50% of wildtype activity ($p<0.001$) (Figure 10). Although non-significant, functional analysis of hsPAPSS2 E10K showed to have 60% functional activity when compared to wild type hsPAPSS2a. Furthermore, expression of hsPAPSS2 M281L showed a modest, but non-significant increase in activity.

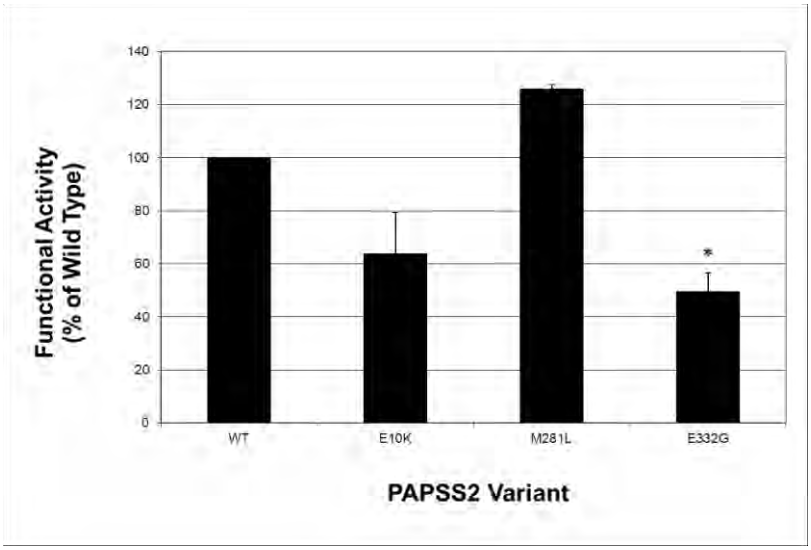

Figure 10: Functional analysis of PAPSS2a genetic variants.

The wild type (WT), E10K, M281L and E332G PAPSS2a genetic variants were over expressed in HEK293 cells. Coexpression of human DHEA sulphotransferase allowed for in vitro conversion of 125nM DHEA to DHEAS. Both DHEA and DHEAS were extracted and measured via thin layer chromatography to determine the percentage of wildtype conversion. PAPSS2a E332G showed significant decrease of 50% of wild type activity. Activities show the mean ±SEM, (n=3) after correction for SULT2A1 alone conversion due to low levels of endogenous PAPSS2a expression. ($p<0.001$)*

4.2.3 Protein expression analysis of pIRES:PAPSS2a/SULT2A1

To determine if the functional differences observed in the hsPAPSS2a variants might be a direct result from the amount of protein expressed within the HEK293 cells, western blot analysis was performed. Protein was extracted from HEK293 cells over expressing the pIRES:hsPAPSS2a/hsSULT2A1 constructs as well as the appropriate controls for each experiment (sections 3.2.4). Western blots were used to detect the amount of hsPAPSS2a and β-actin was used as a loading control (section 3.2.6).

The results showed that the hsPAPSS2a E10K genetic variant had less protein present when compared to the wild type hsPAPSS2a. Similarly, PAPSS2a E332G could only be faintly detected at the protein level. The PAPSS2a M281L showed no difference in protein expression (Figure 11).

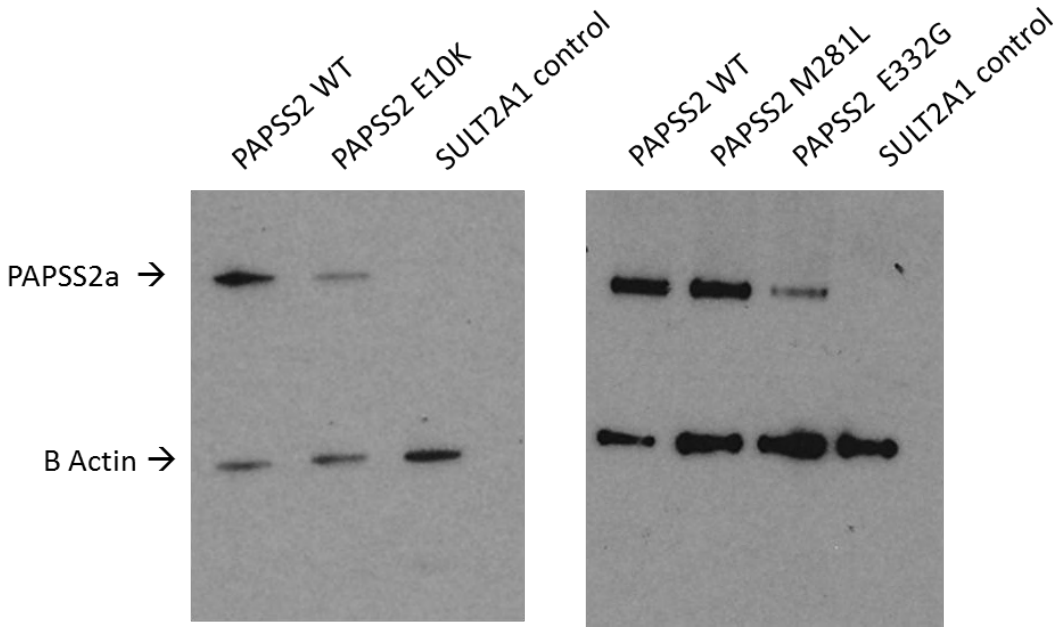

Figure 11: Representative western blots of hsPAPSS2a genetic variants

Levels of expressed PAPSS2a immunoreactive protein in HEK293 cells. Western blots were performed to determine the difference of PAPSS2a variant expression and wild type (WT) protein levels within individual transfection experiments. β actin was used as a loading control Both E10K and E332G PAPSS2a showed to have less immunoreactive protein present when compared to PAPSS2a wild type for individual experiments. M281L PAPSS2a had similar levels of protein when compared to the PAPSS2a wild type (n=1).

4.3 *In silco* analysis of PAPSS2 genetic variants

In silico modelling was performed of PAPSS2 genetic variants to determine how the amino acids changes might alter the overall structure of the protein. At present, the crystal structure for hsPAPSS2 is unknown. Therefore, the current computational model for this protein is based on the hsPAPSS1 solved structure (Harjes et al, 2005). However, PAPSS2a E10K could not be analysed as the model used begins at amino acid 31. In

addition, hsPAPSS2a M281L aligns to a leucine in hsPAPSS1. As the current PAPSS2a model is based on the hsPAPSS1 sequence, it would not provide sufficient information about the disruption of the hsPAPSS2 to analyse M281L using this computation model. Subsequently, of the mutants functionally tested, hsPAPSS2a E332G was the only variant to undergo *in silico* analysis.

In silico modelling of hsPAPSS2a E332 revealed that the glutamic acid is capable of forming hydrogen bonds with an argnine at position 273 and a glutamic acid 274. Alteration of E332 to an uncharged glycine is predicted to disrupt the formation of these hydrogen bonds (Figure 12).

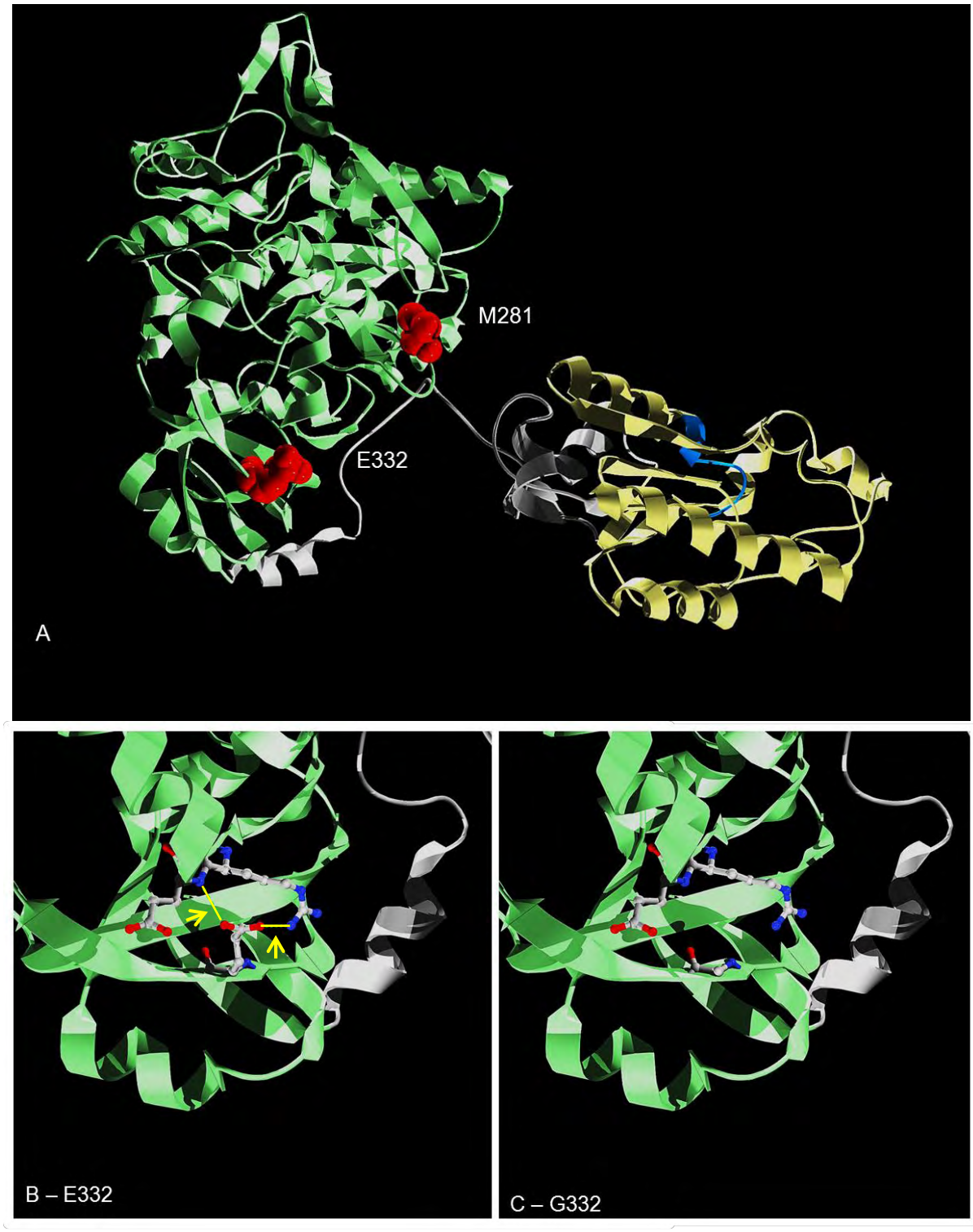

Figure 12: *In silico* modelling of PAPSS2a genetic variants

Figure 12: *In silico* modelling of PAPSS2a genetic variants

Panel A shows the three dimensional locations of PAPSS2a M281 and E332 within the carboxyl ATP sulphurylase domain (green). The APS kinase domain is represented in yellow. The E10K mutation could not be modelled as the predicted model begins as amino acid 31. Panel B shows a close up representation of E332. It is predicted to form hydrogen bonds with R273 and E274 (indicated by the yellow arrows). Panel C shows a representation of the E332G genetic variant. This amino acid change is predicted to disrupt the hydrogen bond formation with R273 and E274. (The radiographic structure of hsPAPSS1 served as the template for modelling wildtype and E332G genetic variant with the use of Swiss-Pdb-Viewer [Swiss Institute of Bioinformatics] and POV-Ray3.6 [POV-Team])

4.4 Generation of HEK293 stable cell lines

Stably transfected HEK293 cells containing pIRES:hsPAPSS2a/hsSULT2A constructs were generated for future assay experiments (section 3.2.3). Generating stably transfected cell lines aimed to eliminate the differences observed in DNA uptake and subsequent protein expression often observed with transient transfections. In total 14 stable HEK293 cell lines were generated including, pIRES:hsPAPSS2a/hsSULT2A1, and pIRES:hsPAPSS1/SULT2A. Furthermore, pIRES vectors with hsPAPSS2a genetic variants (E10L, M281K, V291M, T48R, R329X, S475X, E332G, D370G or A463V) were made in addition to a pIRES:hsSULT2A1 alone, pIRES:hsPAPSS2a alone, and a pIRES:hsPAPSS2-GFP/hsSULT2A1. Each transfection was initially performed in duplicate and the samples were later combined. A control group of cells was used, which underwent the transfection procedure in the absence of DNA to ensure that the lipofectamine did not cause toxicity or cell death.

Antibiotic selection was used to achieve positive selection of cells expressing the transgenes. The pIRES plasmid expressed a geneticin resistance gene to allow survival of the cells in the presence of the antibiotic. The non DNA transfected control cells underwent cell death, confirming that only cells expressing the pIRES transgenes survived (Figure 13).

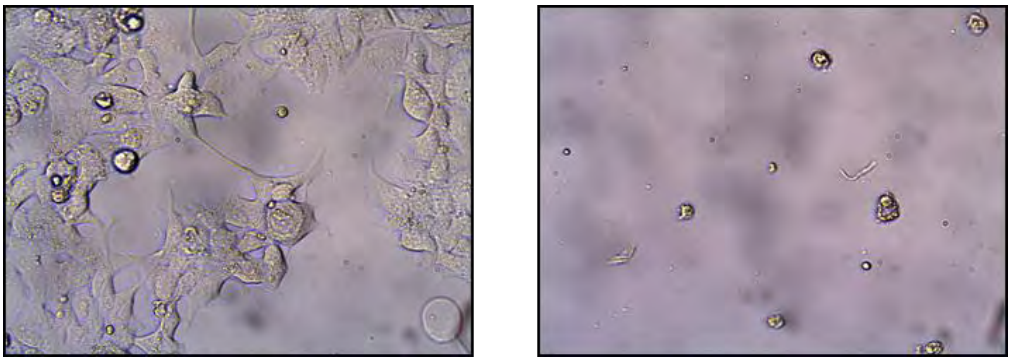

Figure 13: Transfected HEK293 after selection with geneticin

Two days after transfection with pIRES:PAPSS2a/SULT2A1 constructs, HEK293 cells underwent selection with geneticin. After five days of selection cells growing in the presence of the antibiotic confirmed positive expression of the constructs (left panel). A no DNA transfection control (right panel) confirmed cell death in the absence of the pIRES constructs.

5 DISCUSSION

5.1 Characterisation of novel PAPSS2a genetic variants

The aim of this project was to functionally characterise hsPAPSS2a genetic variants in their ability to influence the DHEA to DHEAS sulphation pathway. Several PAPSS2a variants have been previously functionally analysed within the DHEA sulphonation pathway (T48R, R329X and S475X) (Noordam et al., 2009) and the oestrogen pathway (E10K, M281L, V291M and R432K) (Xu et al., 2002). This project has characterised the hsPAPSS2a E332G genetic variant for the first time. This mutation is caused by a single A to G nucleotide change and results in a hydrophilic glycine replacing an glutamic acid within the ATP sulphotransferase domain. This variant showed 50% less activity when compared to wild type hsPAPSS2a. Despite having equal levels of hsPAPSS2a gene expression with wild type hsPAPSS2a, there was a decrease in the level of hsPAPSS2a E332G at the protein level. Therefore, the decrease in functional activity may be directly related to a decrease in stability of hsPAPSS2a E332G protein.

In silico analysis revealed that structurally the E332G variant loses two hydrogen bonds typically formed with nearby amino acids. This structural change may cause the protein to be unstable and rapidly degraded, supporting the decrease of protein detected. However, the resulting amino acid change may also alter the immunospecificity of the hsPAPSS2a antibody. The antibody used was raised against the carboxyl terminal domain of the protein, where the amino acid change is located. This may have caused inefficient detection via western blot. Alternately, the E332G could disrupt the function

of the ATP sulphurylase domain which would support the decrease in functional activity observed.

The frequency of the E332G genetic variant within the human population is yet to be determined as it was identified using the short genetic variation SNP databases (The National Centre for Biotechnology Information). It remains unknown whether a 50% reduction in PAPSS2a would have significant physiological consequences particularly in heterozygous individuals. To date, the only hsPAPSS2a variants known to cause disease are non-functional mutations (Faiyaz ul Haque et al., 1998, Noordam et al., 2009) or ones that have severely decreased activity (6%) (Noordam et al., 2009). It has been suggested that PAPSS activity varies approximately 18 fold in the human liver between individuals (Xu et al., 2001). However, the difference in activity of PAPSS2a in the adrenal glands between individuals is unknown, but it appears likely that a change in functional activity of 50% may only be physiologically significant in homozygous individuals.

5.2 Characterisation of previously analysed PAPSS2a genetic variants

Xu and colleagues (2001) previously assessed the ability of hsPAPSS2a E10K and M281L to sulphonate oestrogen through hsSULT1E1 sulphotransferase. This current project was able to characterise these genetic variants for the first time within the DHEA sulphonation pathway.

hsPAPSS2A E10K results from a single nucleotide change G28A. Despite being non

significant in this study, this mutation showed a tendency to be decrease of 36%. This is comparable to the significant 27.4% decrease observed when analysed in the oestrogen sulphation pathway (Xu et al., 2002). Both studies found a decrease in the function of hsPAPSS2a E10K protein coincided with a decrease of immunoreactive protein. In this current study quantitative real time PCR was used to ensure these results were not from inadequate transfection or gene expression. Each study confirmed protein levels via western blot however, this study used a hsPAPSS2a specific antibody whereas the Xu study detected expression through a His tag. Despite the contrasting detection methods both studies showed a decrease of hsPAPSS2a E10K at the protein level. This suggests that the protein may be unstable and rapidly degraded. Unfortunately, *in silco* analysis could not be performed due to the model lacking this region of protein. However, as E10K is an acidic to basic amino acid change it may cause disruption of ionic bonds and potentially disrupting the PAPSS2a stability.

This project also investigated the functional activity of hsPAPSS2a M281L within the DHEA sulphation pathway. The results showed a slight, nevertheless non-significant increase in hsPAPSS2a M281L activity when compared to wildtype. Western blot analysis revealed that there was no increase of hsPAPSS2a M281L at the protein level. In comparison, hsPAPSS2a M281L previously showed a non significant increase in activity when investigated in the oestrogen sulphation pathway despite no change at the protein level (Xu et al., 2002). Although this increase is not addressed in the paper, it supports the increase observed in this study.

As mentioned previously, alignment of hsPAPSS2a with hsPAPSS1 revealed that M281 of PAPSS2a aligns with L291 of PAPSS1 (Strott, 2002). Therefore, due to the high homology between the two isoforms (77%) (Strott, 2002), it would be expected that a change to a lucine in hsPAPSS2a would not have significant consequences on functional activity. However, it has been shown that hsPASS2a and hsPAPSS1 a capable of forming heterodimers, which may be the mechanism of explaining how hsPAPSS2a relocates to the nucleus in the presence of PAPSS1 (Grum et al., 2010, Besset et al., 2000). When looking at the predicted interface between the two isoforms, M281 of hsPAPSS2a is predicted to be involved at the dimerisation site (Grum et al., 2010). Further studies investigating the APS kinase activity of different PAPS synthase dimers revealed that a heterozygous dimer of hsPAPSS1 and hsPAPSS2a has increased activity when compared to a homozygous hsPAPSS2a dimer (Grum et al., 2010). Therefore, it is hypothesised that hsPAPSS2a M281L may enhances dimerisation formation, subsequently stabilise hsPAPSS2a and increase the activity of the APS kinase domain.

6 CONCLUSIONS AND FUTURE DIRECTIONS

The aim of this project was to characterise the functional ability of hsPAPSS2a and its variants in their ability to allow sulphation of DHEA to DHEAS. In this project three PAPSS2a genetic variants were characterised within the DHEA sulphation pathway. This project functionally assessed the hsPAPSS2a E332G variant for the first time. This protein was observed to have 50% functional activity of hsPAPSS2a wild type. This result has important clinical relevance as it suggests that patients presenting with androgen excess should be screened for this mutation. Furthermore, this study also characterised the hsPAPSS2a E10K and M281L variants within the DHEA sulphation pathway. Although both these variants showed non significant changes in functional activity, both reflected results observed when previously characterised within the oestrogen sulphation pathway.

Further characterisation of the genetic variants not investigated in this study is still required. It will be interesting to determine functional activity of uncharacterised variants as well as those previously analysed with hsSULT1E1. Generation of the pIRES:hsPAPSS2a genetic variant/hsSULT2A1 stable HEK293 cell lines will provide a useful tool for future analysis. It is hoped that these stable lines will eliminate the differences observed between transient transfections and therefore give a more accurate representation of their true functional activity. Furthermore, the HEK293 expressing pIRES:hsPAPSS2a-GFP/hsSULT2A1 will allow for future investigation into the cellular

localisation of hsPAPSS2a and how over expression of disrupted hsPAPSS2a protein may alter its position within the cell. This work will aid in determining if the cellular localisation is important feature of regulating hsPAPSS2a function and subsequent sulphonation of molecules.

Determining why different hsPAPSS2a genetic variants result in a range of clinical phenotypes will be an important aspect of this research. Over expression of hsPAPSS2a genetic variants *in vitro* in conjunction with different sulphotransferases (SULT2A1 or SULT1E1) will highlight if PAPSS2 variants have varying activities in the sulphation pathway. Furthermore, these future studies will provide insights into how hsPAPSS2a variants impact on a given physiological phenotype, such as the previously observed androgen excess or bone dysplasia. Therefore, this will hopefully provide a basis for improving the clinical management of PAPSS2 deficient individuals.

Investigating the role of vitamin D in inflammation related muscle loss

ALIESHA GRIFFIN

Project Two

This project is submitted in partial fulfilment of the requirements for the award of the Masters of Medical Research

Centre for Endocrinology Diabetes and Metabolism

School of Clinical and Experimental Medicine

Institute of Biomedical Research

University of Birmingham

August 2011.

ABSTRACT

Background: Rheumatoid arthritis (RA) is an autoimmune disease that results in inflammation of the synovial joints, loss of bone mass and muscle loss. Inflammatory related skeletal muscle wasting increases the risk of falls and fractures and the mortality and morbidity of patients. There is evidence to suggest that low levels of vitamin D also correlate with muscle weakness and loss. This is supported by observations that vitamin D has an important role in skeletal muscle development and function.

Aim: The aim of this project was to determine if inflammatory related muscle atrophy is directly mediated through impaired vitamin D actions or its metabolism.

Methods: Murine C2C12 myoblasts were differentiated over a six day period and treated with TNFα, IL-6 and IL-1β for 24 hours. Alternatively, C2C12 myoblasts were differentiated for six days in media preconditioned with serum from human RA synovial fibroblasts. Quantitative real time RT-PCR was used to determine changes in the mRNA levels of the vitamin D receptor and mRNA for gene involved in vitamin D metabolism.

Results: Treatment of C2C12 muscle cells with pro-inflammatory or with pre conditioned media from synovial fibroblasts did not cause any changes in gene expression of the vitamin D receptor or the genes responsible for vitamin D activation or catabolism.

Conclusion: It is concluded from this study that inflammatory related muscle atrophy is not a direct result of changes in vitamin D actions through its receptor or its metabolism.

ACKNOWLEDGEMENT

I would like to thank my supervisor Dr. Mark Cooper for giving me guidance and assistance throughout this study. I am appreciative of his valuable advice and continued enthusiasm for this project. I am also grateful to Dr. Rowan Hardy for his initial ideas and support in the development of the project. I would also like to acknowledge Dr. Stuart Morgan for his continued assistance with the laboratory work and helpful feedback during this project.

TABLE OF CONTENTS

7 INTRODUCTION 48

7.1 Rheumatoid arthritis and muscle wasting 48

7.2 Inflammatory cytokines and their effects on skeletal muscle 49

7.3 Vitamin D physiology 51

7.3.1 Classical Vitamin D actions 54

7.3.2 Non-classical actions of vitamin D 54

7.4 Vitamin D and skeletal muscle 55

7.5 Vitamin D and Rheumatoid Arthritis 57

8 PROJECT AIMS AND HYPOTHESIS 59

9 MATERIALS AND METHODS 60

9.1 Cellular Biology 60

9.1.1 Mammalian Cell Culture 60

9.1.2 Cytokine treatment of differentiated C2C12 cell line 61

9.1.3 Serum conditioned media treatment of C2C12 myoblasts 61

9.1.4 Differentiation of C2C12 in the presence of 1,25(OH)$_2$D$_3$ 62

9.2 Molecular Biology 62

9.2.1 RNA extraction 62

9.2.2 Reverse Transcription 63

9.2.3 Quantitative Real Time RT-PCR 63

9.2.4 Quantification of Nucleic Acids 64

10 RESULTS 66

10.1 Characterisation of C2C12 myogeneis 66

10.2 Characterisation of Vitamin D effects on C2C12 68

10.3 Effects of inflammatory cytokines on C2C12 myofibres 72

10.3.1 TNFα, IL-6 and IL-1β treatment of C2C12 myofibres 72

10.3.2 Differentiation of C2C12 myofibres in preconditioned media 77

10.4 Vitamin D effects on muscle differentiation 81

11 DISCUSSION 84

11.1 Vitamin D actions and metabolism in C2C12 cells 84

11.2 Inflammatory cytokines effects of vitamin D metabolism 85

11.3 Modelling inflammatory related muscle atrophy in C2C12 myofibres. 86

11.4 Indirect effects of Vitamin D on inflammatory related muscle atrophy 88

11.5 Vitamin D and muscle differentiation 89

12 CONCLUSIONS AND FUTURE DIRECTIONS 91

TABLE OF FIGURES

Figure 14: Vitamin D metabolism in humans. 53
Figure 15: Morphological changes of C2C12 myoblasts during differentiation 66
Figure 16: Gene expression of myogenin, myostatin and myo D during C2C12 muscle differentiation. 68
Figure 17: Gene expression of muVDR, muCyp24A1 and muCyp27B1 during C2C12 muscle differentiation. 69
Figure 18: Gene expression of muVDR, muCyp24A1 and Cyp27B1 in response to vitamin D treatment. 71
Figure 19: Cell morphology in day six treated C2C12 after treatment. 73
Figure 20: Gene expression of muVDR, muCyp24A1 and Cyp24B1 in response to inflammatory cytokine treatment. 74
Figure 21: Gene expression of muMAFbx and muMuRF1 after 24 hour treatment with inflammatory cytokines. 76
Figure 22: Gene expression of muVDR, muCyp24A1 and Cyp24B1 in response to differentiation in the presence of preconditioned media. 78
Figure 23: Gene expression of myostatin and myogenin in response to differentiation in the presence of preconditioned media. 79
Figure 24: Gene expression of MuRF1 and MAFbx in response to differentiation in the presence of preconditioned media. 81
Figure 25: Gene expression of myo D, myogenin and myostatin in response to differentiation of C2C12 myoblasts in the presence of vitamin D. 83

LIST OF ABBREVIATIONS

24-OHase	25-hydroxyvitamin D_3 24-hydroxylase
25-OHase	25-hydroxylase
AU	arbitrary units
cDNA	complementary DNA
DMEM	Dulbecco's Modified Eagle's medium
IL-1β	interleukin 1β
IL-6	interleukin 6
MAFbx	Atrogin 1/muscle atrophy F-box
MuRF1	Muscle Ring Finger 1
PBS	phosphate buffered saline
RA	Rheumatoid arthritis
rh	recombinant human
rm	recombinant murine
RT-PCR	Reverse Transcriptase Polymerase Chain Reaction
TNFα	tumour necrosis factor α
VDR	vitamin D receptor
VDRE	vitamin D response element

7 INTRODUCTION

7.1 Rheumatoid arthritis and muscle wasting

Rheumatoid arthritis (RA) is a systemic inflammatory autoimmune disorder where patients primarily suffer from inflammation of the synovial joints. The disease results in an erosive arthritis with destruction of the joints, a loss of bone mass, as well as local and systemic muscle wasting. This disorder has a multifactorial aetiology in which both genetic and non-genetic components are believed to be contributing factors (McInnes and Schett, 2007). The cause of the initiation of the inappropriate immune response in RA is unknown. However, there is a growing body of support suggesting that vitamin D homeostasis has a role in the development of this disease.

RA is characterised by an infiltration of immune cells into the synovial joints. These immune cells are also capable of causing damage to the surrounding tissue, including muscle and bone (McInnes and Schett, 2007). Clinical studies have observed that RA patients suffer significant muscle wasting as a result of this inflammation (Helliwell and Jackson, 1994). In addition, it has been observed that muscle wasting is more prevalent in RA patients than in the general population (Matschke et al., 2010). Subsequently, patients often have a range of complications including an increased risk of falling and fractures as well as further development of joint degradation through reduced use (van Staa et al., 2006). This highlights that muscle wasting, in addition to synovial joint destruction, is a serious and common characteristic of this disease.

Skeletal muscle atrophy often occurs in response to starvation, disuse, cancer, aging and chronic inflammatory diseases. It results in decreased muscle mass, muscle weakness, fatigue and contributes to the mortality and morbidity associated with the primary illness (Firestein, 2003). Muscle atrophy is characterised by a reduction in muscle fibre diameter, force output and fatigue resistance (Jackman and Kandarian, 2004). Within the muscle fibre there is a decrease in protein synthesis as well as an increase in expression of protein breakdown pathways such as the ubiquitin-proteasome pathway (Glass, 2003). It is well established that inflammatory cytokines increase the rate of muscle catabolism and subsequent muscle wasting in RA and other pathological inflammatory conditions (McInnes and Schett, 2007).

7.2 Inflammatory cytokines and their effects on skeletal muscle

Skeletal muscle mass is maintained through a balance between protein synthesis and protein degradation. Inflammation is a well-known cause of muscle atrophy as it accelerates protein degradation and decreases protein synthesis. Pro-inflammatory cytokines, such as interleukin 6 (IL-6), interleukin 1β (IL-1β) and tumour necrosis factor α (TNFα) are associated with the depletion of fat stores and loss of muscular tissue (Argiles and Lopez-Soriano, 1999). In many human diseases involving high muscle catabolism, such as RA, muscle loss is often reported in conjunction with elevated levels of these pro-inflammatory cytokines (McInnes and Schett, 2007).

Atrophying muscles have an increase in protein degradation, which primarily occurs

through the E3 ubiquitin-proteasome pathway (Jagoe and Goldberg, 2001). The muscle-specific ubiquitin ligases atrogin 1/muscle atrophy F-box (MAFbx) and Muscle Ring Finger 1 (MuRF1) are induced during muscle atrophy and contribute to protein breakdown (Sandri, 2008). Pro-inflammatory cytokines, such as TNFα, IL-6 and IL-1β, are capable inducing muscle catabolism through this pathway.

TNFα is known to increase the expression of MAFbx in skeletal muscle (Li et al., 2005). Exogenous TNFα is reported to stimulate protein degradation in differentiating myoblasts (Li et al., 1998) and in *in vivo* experimental animal models (Garcia-Martinez et al., 1993). Another suggested mechanism of action is that TNFα promotes muscle atrophy through activation of the NFκB pathway (Li et al., 1998) which in turn supresses key muscle differentiation genes at the post transcription level (Guttridge et al., 2000).

IL-1β is also known to be involved in skeletal muscle atrophy. *In vivo* experiments in rats confirmed that MuRF1 and MAFbx were up regulated after treatment with IL-1β (Bodine et al., 2001). Additional studies showed IL-1β treatment of rats was able to reduce the synthesis of major skeletal muscle proteins (Cooney et al., 1999). *In vitro* experiments confirmed that IL-1β stimulates catabolism in C2C12 myofibres through increases in both MuRF1 and MAFbx expression (Li et al., 2009). This highlights that IL-1β has a key role in inflammatory related skeletal muscle atrophy.

The pro-inflammatory cytokine IL-6 can also directly induce skeletal muscle atrophy. Mice infused with IL-6 had a significant decrease in muscle protein after two weeks

(Haddad et al., 2005). This is mediated, at least in part, by an up regulation of MAFbx expression (Baltgalvis et al., 2009). Additionally, IL-6 activates pathways which in turn down regulate growth factor-mediated intracellular signalling mechanisms (Haddad et al., 2005). Therefore, IL-6 is also capable of contributing to muscle atrophy in chronic inflammatory diseases via several pathways.

7.3 Vitamin D physiology

The term vitamin D (calciferol) refers to two steroids: vitamin D_2 (ergocalciferol) and vitamin D_3 (cholecalciferol). For humans, the major source of vitamin D comes from the synthesis of vitamin D_3 as a result of sun exposure on the skin. Photochemical synthesis from the sun's UVB radiation (280-320nm) is capable of converting provitamin D_3 (7-dehydrocholesterol) present in the skin to previtamin D_3. This is then further converted in the epidermal basal layers to vitamin D_3 (Deeb et al., 2007). Consequently, vitamin D_3 levels can be reduced with dark pigmented skin, the use of sunscreen or clothing and in housebound elderly populations. Both vitamin D_2 and D_3 can be obtained through dietary intake or supplements (Lips, 2006). However, dietary intake is often insufficient as it supplies only 20% of the required amount (Wen and Baker, 2011). Vitamin D_2 and D_3 have differing side chains and both require further conversion to generate the active vitamin D metabolites (Figure 14).

Once vitamin D_3 is generated in the skin, it is transported to the liver where it is hydroxylated by 25-hydroxylase (25-OHase) generating 25-hydroxycholecalciferol

(25[OH]D_3). The 25-OHase enzyme is encoded by the *CYP27A1* gene which is expressed in liver mitochondria and microsomes (Deeb et al., 2007). The subsequent step in the metabolism of vitamin D involves the 25-hydroxyvitamin D_3-1α-hydroxylase (1α-OHase) enzyme. This enzyme is expressed in the kidney and is encoded by the *CYP27B1* gene. This hydroxylase catalyses the reaction of 25(OH)D_3 to calcitriol (1α,25[OH_2]D_3); the most active metabolite of vitamin D. The *CYP27B1* gene is a key regulator of vitamin D action in the body and is tightly controlled by parathyroid hormone, calcium, phosphate and 1α,25(OH_2)D_3 (Lips, 2006).

24-hydroxylation of 1α,25(OH_2)D_3 and 25(OH)D_3 by 25-hydroxyvitamin D_3 24-hydroxylase (24-OHase) generates the inactive forms of vitamin D_3; 24,25(OH)2D_3 and 1α,24,25$(OH)_2D_3$. These metabolites are then excreted by the body. 24-OHase is encoded by *CYP24A1* gene and is the rate limiting step in the catabolism of 25(OH)D_3 and 1α,25(OH)2D_3 (Deeb et al., 2007). *CYP24A1* is primarily expressed in the kidneys and is typically regulated by 1α,25(OH_2)D_3 to reduce the amount of active vitamin D as well as its metabolites 24,25(OH)2D_3 and 1α,24,25$(OH)_2D_3$ (Lips, 2006).

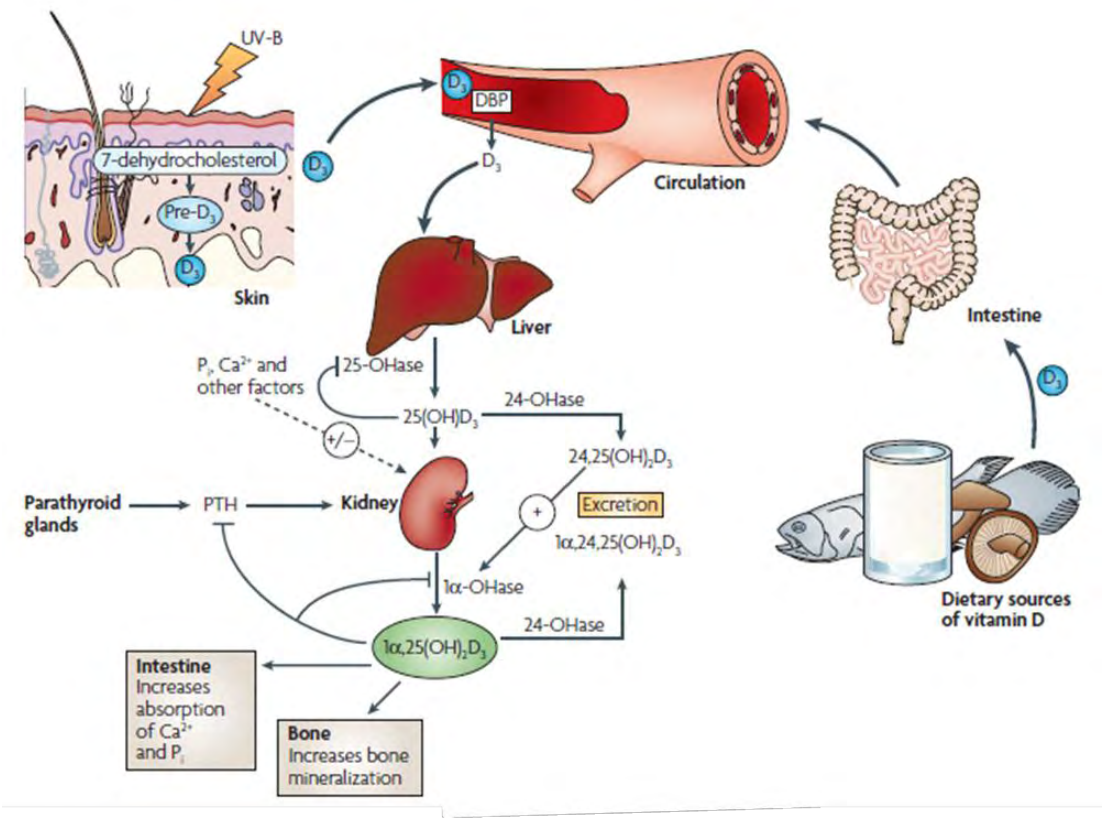

Figure 14: Vitamin D metabolism in humans.

Initially, the provitamin D_3 (7-dehydrocholesterol) is converted to the previtamin D_3 in response to ultraviolet B (sunlight) exposure in the skin. This is then further converted to vitamin D_3 in the epidermal basal layers. Vitamin D_3 from the skin or absorbed by the intestine from dietary intake binds to vitamin D-binding protein (DBP) in the bloodstream, and is transported to the liver. In the liver vitamin D_3 is hydroxylated by 25-hydroxylase (25-OHase) generating 25-hydroxycholecalciferol (25[OH]D_3). Subsequently 25(OH)D_3 is 1α-hydroxylated in the kidney by 25-hydroxyvitamin D3 -1α-hydroxylase (1α -OHase). This generates the active steroid 1α,25(OH_2)D_3 which has various effects on target tissues throughout the body. 25(OH)D_3 and 1α,25(OH_2)D_3 are catabolised by 24-hydroxylation by 25-hydroxyvitamin D 24-hydroxylase (24-OHase). The resulting metabolites 24,25(OH)D_3 and 1α,24,25$(OH)_2D_3$ are excreted by the body. (adapted from Deeb et al., 2007).

7.3.1 Classical Vitamin D actions

Genomic actions of vitamin D are initiated by $1\alpha,25(OH_2)D_3$ binding to the vitamin D receptor (VDR). The VDR acts as a heterodimer and typically binds to the retinoid X receptor. This complex is capable of recognising vitamin D response elements (VDREs) in promoter regions in order to up regulate or repress gene transcription (Bikle, 2009). Vitamin D influences target organs such as bone, intestine, kidneys and parathyroid glands. Classically, vitamin D stimulates expression of proteins involved in calcium and phosphate homeostasis as well as bone mineralisation (Ceglia, 2008). Impaired vitamin D action, such as vitamin D deficiency or genetic defects in the vitamin D activating genes can result in severe disease. Children often suffer from the bone softening disorder rickets, while adults present with osteomalacia often characterised by hypocalcaemia and hypophosphataemia with secondary hyperparathyroidism and bone abnormalities (Endo et al., 2003). This emphasises the fact that vitamin D is essential for adequate phosphate and calcium regulation and correct bone formation in humans.

7.3.2 Non-classical actions of vitamin D

The VDR is known to be expressed in a wide range of tissues unrelated to calcium and bone metabolism. Discovery of moderate expression levels of the VDR in nearly all tissues, including skeletal muscle, suggests vitamin D has a range of actions throughout the body (Holick, 2007). Recently, vitamin D has been linked with the regulation of hormone secretion, including insulin and parathyroid hormone, as well as modifying cellular proliferation and differentiation *in vitro* (Bikle, 2009). Furthermore, vitamin D

can regulate immune function by inhibiting pro-inflammatory macrophage derived cytokines such as interleukin 12, IL-1β, IL-6 and TNFα (Bikle, 2009). This supports the premise that vitamin D is capable of exerting non-classical effects across many tissues in the body.

In addition to regulating gene transcription, $1\alpha,25(OH_2)D_3$ is also capable of initiating rapid non genomic effects within cells. The mechanism behind this action remains to be fully characterised. $1\alpha,25(OH_2)D_3$ may bind a novel receptor or the VDR which has been translocated to the cell membrane. After binding this receptor, vitamin D activates second messenger pathways resulting in instant cellular effects, such as rapid calcium uptake in muscle cells (Ceglia, 2008).

7.4 Vitamin D and skeletal muscle

Currently there is new interest in the relationship between vitamin D and muscle function. Identification of the VDR within skeletal muscle tissue provides evidence that vitamin D may have a direct effect on this tissue (Bischoff et al., 2001). However, the effect of $1,25(OH)_2D_3$ on skeletal muscle remains unclear. $1,25(OH)_2D_3$ can influence muscle calcium uptake, phospholipid metabolism, phosphate transport across the cell membrane and muscle cell proliferation and differentiation. $1,25(OH)_2D_3$ regulates calcium uptake *in vitro* and *in vivo* which subsequently controls muscle function through influencing its contraction and relaxation properties (Ceglia, 2008). Additionally, treatment of myoblasts with vitamin D has a mitogenic effect during proliferation, and

inhibits proliferation during myofibre differentiation (Drittanti et al., 1989). Thus, vitamin D may play an important role in skeletal muscle development and function.

Animal models have provided additional evidence that vitamin D has a positive effect on muscle maturation and strength. Muscle fibres in vitamin D receptor knock-out mice are significantly smaller and are more variable in size than wild type controls. This suggests that the VDR plays a key role in skeletal muscle fibre development and its maturation (Endo et al., 2003).

In humans, vitamin D deficiency can cause skeletal muscle atrophy of varying severity. Several clinical studies show that vitamin D has a key role in skeletal muscle and metabolism and that muscle weakness followed by atrophy is a common symptom of vitamin D deficiency (Pfeifer et al., 2002). Low $25(OH)D_3$ levels (the accepted measure of vitamin D body stores) are associated with an increased risk of repeated falling and fractures (Snijder et al., 2006). Additionally, adult patients with profound vitamin D deficiency show predominantly type II muscle atrophy (Ceglia, 2008). These muscle fibres are fast-twitch and are the first muscles to be engaged in the prevention of falls. Treatment of low $25(OH)D_3$ with either Vitamin D_3 on its own (Bischoff-Ferrari et al., 2009) or in a combination with calcium (Bischoff et al., 2003, Pfeifer et al., 2009) is capable of reducing the risk of falls. Vitamin D_2 supplementation in combination with calcium has also shown similar outcomes (Flicker et al., 2005). Alternately, other studies did not observe any significant increase in muscle strength (Verreault et al., 2002, Stockton et al., 2011). One study in particular identified an increased incidence of falls

following supplementation with vitamin D in elderly women (Sanders et al., 2010). Although the evidence is inconsistent, it is suggested that treatment with vitamin D might aid improvement of musculoskeletal health in individuals with disease related muscle atrophy.

7.5 Vitamin D and Rheumatoid Arthritis

Based on several recent clinical and laboratory studies there has been an increased interest in vitamin D in the treatment and pathogenesis of RA. Currently, there have been several observations that link vitamin D and RA. Initially, epidemiological studies proposed an association between vitamin D deficiency with a susceptibility to developing the disease (Wen and Baker, 2011). Secondly, a decreased concentration of $25(OH)D_3$ in the blood can be a risk factor for the initiation of RA (Merlino et al., 2004). Similarly, a dysfunctional VDR is related to poor bone development and health, as well as an increased risk of chronic diseases including RA (Holick, 2007). Finally, several studies concluded that low levels of $25(OH)D_3$ was more likely to be associated with enhanced inflammation, pain and fatigue (Cutolo et al., 2007, Kroger et al., 1993). These observations highlight the idea that vitamin D may have a role in the development, pathogenesis or treatment of RA.

Interestingly, the VDR is expressed within endothelial cells within rheumatoid lesions, although it is not expressed in normal healthy synovium. Tetlow et al (1999) have reported that more cells in the RA synovium express the VDR compared to controls. This

further supports the idea that vitamin D may play an important role within the pathophysiology of RA.

8 PROJECT AIMS AND HYPOTHESIS

Given the reported positive effects of vitamin D on muscles, we hypothesised that muscle wasting in patients with autoimmune inflammatory diseases (such as RA) occurs as a direct result of impaired vitamin D action or metabolism. This project aimed to clarify the potential role of vitamin D in inflammation associated muscle loss by addressing the following objectives:

- Characterise the expression of the *VDR*, and vitamin D metabolism genes *Cyp27B1* and *Cyp24A1* during differentiation of muscle cells.
- Examine the effects of the major inflammatory cytokines TNFα, IL-6 and IL-1β on the expression of *VDR*, and vitamin D metabolism genes *Cyp27B1* and *Cyp24A1* within mouse myofibres.
- Examine the effects of increasing concentrations of vitamin D in regulating muscle proliferation and differentiation of myoblasts to myofibres.

9 MATERIALS AND METHODS

9.1 Cellular Biology

9.1.1 Mammalian Cell Culture

This study used the C2C12 skeletal muscle cell line, which were originally isolated through serial passage of myoblasts cultured from the thigh of C3H mice inflicted with crush injury (Yaffe and Saxel, 1977). These cells are capable of differentiating from pluripotent myoblasts to fully differentiated myofibres when grown in the presence of horse serum. C2C12 mouse myoblasts were cultured in high glucose Dulbecco's Modified Eagle's medium (DMEM) with L-glutamine. Complete growth media was supplemented with 10% foetal bovine serum (Sigma) and 1% penicillin (5 U/mL) streptomycin (5 µg/mL) (Invitrogen). Cells were maintained with 5% CO_2 at 37ºC in a humidified incubator and passaged at 70% confluence. Cells were harvested by trypsin-EDTA digestion.

Cells used for assays were passaged into 12-well plates. Once cells reached 80% confluence, differentiation of C2C12 myoblasts to myofibres was induced by replacing complete growth media with differentiation media. Differentiation media consisted of DMEM with L-glutamine supplemented with 5% horse serum, 1% penicillin (5 U/mL) and streptomycin (5µg/mL) (Invitrogen). During differentiation media was replaced every two to three days.

9.1.2 *Cytokine treatment of differentiated C2C12 cell line*

Day six differentiated C2C12 myofibres were treated with the inflammatory cytokines recombinant murine (rm) TNFα and IL-6 and recombinant human (rh) IL-1β (R&D Systems) and $1,25(OH)_2D_3$ (Enzo Life Sciences). Prior to treatment, cells were briefly washed with serum free DMEM and incubated in serum-free media for four hours. Subsequently, cells were placed in fresh serum-free media in the presence of 10ng/mL rmTNFα (stock 10µg/mL in 0.1% bovine serum albumin in phosphate buffered saline [PBS]), 25ng/mL rmIL-6 (stock 2.5µg/mL in PBS), 10ng/mL rhIL-1β (stock 10µg/mL in PBS) or with 10nM $1\alpha,25(OH_2)D_3$ (stock 10µM in 100% ethanol). Each assay was performed in duplicate.

Cells were incubated for 24 hours at 37ºC in a 5% CO_2 humidified incubator prior to harvesting. For harvesting, the media was removed, cells were washed with 1mL of PBS and TRI Reagent (Sigma) was added for RNA extraction (section 3.1.6).

9.1.3 *Synovial fibroblast serum-conditioned media treatment of C2C12 myoblasts*

Undifferentiated C2C12 myoblasts were passaged into 12-well plates and allowed to reach 80% confluence prior to differentiation. Differentiation media was supplemented with serum extracted from human synovial fibroblast cells. These fibroblast cells were harvested from a single RA patient, cultured and received treatment with TNFα, dexamethasone or no treatment prior to the serum being harvested. Each assay was performed in duplicate. The media was changed on day three of differentiation and

replaced with fresh serum-conditioned media. On day six of differentiation the cells were harvested in TRI Reagent (Sigma) for RNA extraction (section 3.1.6).

9.1.4 Differentiation of C2C12 in the presence of $1,25(OH)_2D_3$

Undifferentiated C2C12 myoblasts were passaged into 12-well plates and allowed to reach 80% confluence prior to differentiation. Differentiation media was supplemented with either 1nM, 10nM or 100nM of $1,25(OH)_2D_3$ (Enzo Life Sciences). Initially a 1:1000 dilution followed by a 1:10 serial dilution was performed to make the supplemented media from a 100µM $1,25(OH)_2D_3$ stock (in 100% ethanol). The media was changed on day three of differentiation and replaced with fresh $1,25(OH)_2D_3$ supplemented media at the appropriate concentration. Each assay was performed in duplicate. Cells were harvested at day one, day three and day six of differentiation in TRI Reagent (Sigma) for RNA extraction (section 3.1.6).

9.2 Molecular Biology

9.2.1 RNA extraction

RNA extraction is a procedure which allows for the isolation of RNA from a biological sample and therefore gives a snapshot of the genes being actively transcribed at that time point. RNA was isolated from C2C12 cells using TRI Reagent (Sigma). Typically, cells were washed with 1mL in PBS (Sigma) before 1mL of TRI Reagent was added. Pipetting was used to dislodge cells before the cell suspension was placed in a 1.5mL

microcentrifuge tube. 200µL of chloroform was added to the samples and they were mixed vigorously. Samples were incubated at room temperature for 10 minutes and centrifuged at 13,000rpm for 20 minutes at 4ºC. The upper aqueous phase containing the RNA was transferred to a fresh 1.5mL tube. The RNA was precipitated using 500µL of cold isopropyl alcohol. Samples were incubated for at least 20 minutes at -20ºC. The RNA was pelleted by centrifugation at 13,000rpm for 10 minutes at 4ºC and washed in 70% ethanol, followed by a further centrifugation step at 13,000rpm from 10 minutes at 4ºC. RNA was eluted into RNase-free water, quantified (section 3.1.3) and stored at -20ºC.

9.2.2 Reverse Transcription

Reverse transcription is a methodology that allows for the generation of complementary DNA (cDNA) from a purified RNA sample. cDNA was prepared from total RNA using TaqMan Reverse Transcriptase kit according to the manufactures instructions (Applied Biosystems). Typically 20µL reactions were made containing; 1X reaction buffer, 5.5mM magnesium chloride, 500µM of each dNTP, 2.5µM of random hexamer primers, 0.4U/µL of RNase Inhibitor, 1.25U/µL Mulitscribe Reverse Transcriptase and 700ng of RNA. Samples were subjected to 25ºC for 10 minutes, 37ºC for one hour, 48ºC for 30 minutes and 95ºC for five minutes in a thermal cycler. Samples were stored at -20ºC.

9.2.3 Quantitative Real Time RT-PCR

Real time Reverse Transcriptase Polymerase Chain Reaction (RT-PCR) is a method

which allows for amplification and simultaneous quantification of specific genes of interest. A fluorescent reporter probe method was used where probes were tagged with the FAM reporter. Typically, 10µL reactions were made consisting of 0.5µL of Assay on Demand (Applied Biosystems) for either murine *myoD*, *myogenin*, *myostatin*, *VDR*, *Cyp24A1*, *Cyp27B1*, *MAFbx32*, or *MuRF1*, 5µL of TaqMan Master Mix (Applied Biosystems) and 4.5µL of previously prepared cDNA (section 3.1.7). Similarly, 18S expression was also analysed using a 0.5µL VIC labelled report probe (Applied Biosystems) with 5µL of TaqMan Master Mix (Applied Biosystems) and 4.5µL of previously prepared cDNA.

Samples were prepared in 96 well Optical Reaction Plates (Applied Biosystems) and sealed with adhesive PCR film (Thermo scientific). Reactions were run on an ABI Prism SDS 7500 Thermocycler for 50ºC for two minutes, 95ºC for 10 minutes, followed by 40 cycles of 95ºC for 15 seconds and 60ºC for one minute. Samples were analysed using 7500 System SDS software (Applied Biosystems).

9.2.4 Quantification of Nucleic Acids

Purified plasmids and extracted RNA were all quantified using the NanoDrop® ND-1000 spectrophotometer. Typically, distilled water was used to determine a background level and then 1.5µL of sample was applied onto the spectrophotometer. For nucleic acid samples a ratio of A260/280 was used to determine purity. A ratio between 1.8 and 2.2 was considered acceptable indicating RNA could be used in future experiments.

9.2.5 Statistical Analysis

All experiments were conducted in duplicate, with each duplicate representing n=1. Arbitrary units (AU) were used to display gene mRNA expression data as ± standard error of the mean (SEM). Means were compared against each other by using an unpaired (two-tailed) students t-test, whilst multiple means were compared by analysis of variance (ANOVA) Post Hoc Dunnet (two-sided) test. $P<0.05$ was considered to be statistically significant.

10 RESULTS

10.1 Characterisation of C2C12 myogeneis

Murine C2C12 myoblasts are a well established *in vitro* model for investigating the differentiation of myoblasts (mononucleated myogenic cells) to myofibres (multinucleated cells). During myogenesis, proliferating myoblasts withdraw from the cell cycle, obtain an apoptosis-resistant phenotype and fuse into myofibres (Figure 15). Changes in gene expression of myogenic regulatory factors accompany the differentiation of myoblast to myofibres.

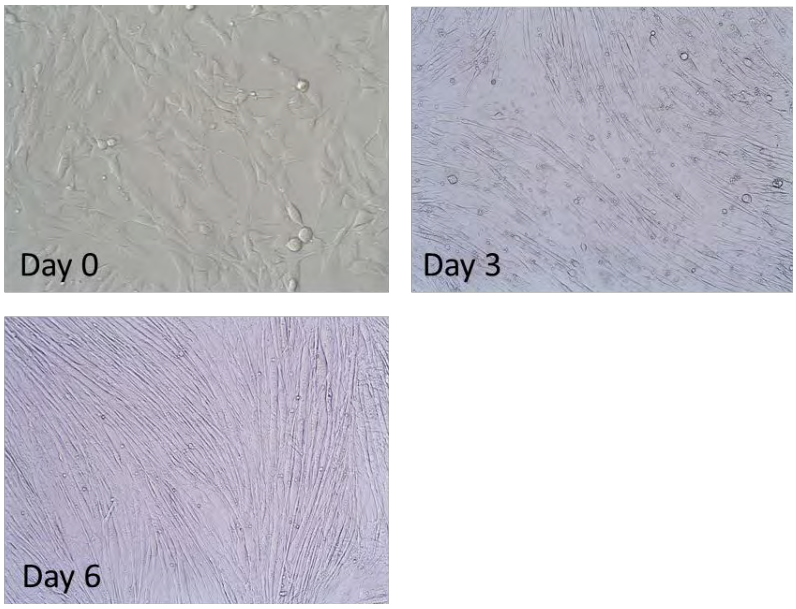

Figure 15: Morphological changes of C2C12 myoblasts during differentiation

Murine C2C12 myoblast differentiation was induced by supplementing culture media with 5% horse serum. Day zero depicts multipotent C2C12 myoblasts. Over six days of differentiation the C2C12 cells stop proliferating and fuse together to form muti-nucleated myofibres.

In order to characterise differentiation of the C2C12 cell line, expression of murine MyoD, myogenin and myostatin was examined. MyoD is a transcription factor which marks muscle differentiation. It halts proliferation and indicates the cells commitment to the myoblast lineage. Secondly, myogenin is a transcription factor which is essential for muscle development. Finally, myostatin is an inhibitor of muscle growth and differentiation. To induce myogenesis of the C2C12 myoblasts, growth media was replaced with differentiation media. Cells were harvested at the myoblast stage (day zero), day three and day six of myogenesis for gene expression analysis using quantitative real time RT-PCR (section 9.2.3).

Over six days of differentiation, there was a significant increase in the expression of myogenic regulatory factors myogenin, myostatin and myoD (Figure 16). Myostatin had a 150 fold up regulation during differentiation by increasing from 0.0002 AU ±1.1E-5 to 0.03AU ±0.001 ($p<0.05$). Similarly, myogenin showed an up regulation in expression, increasing 0.24AU ±0.1 to 187AU ±46.8 ($p<0.05$). Additionally, myoD had a similar expression pattern, displaying a 27 fold up regulation from 0.47AU ±0.04 to 12.8AU ±4.3 ($p<0.05$).

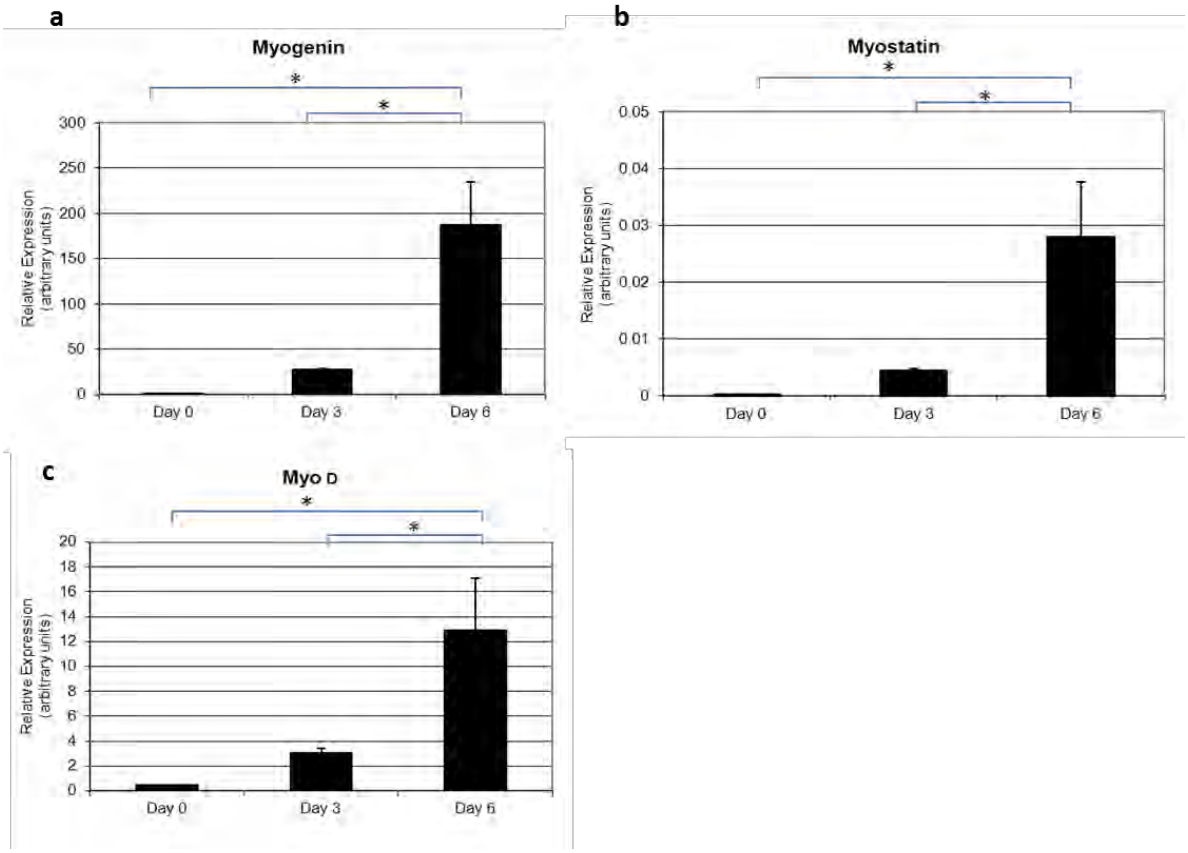

Figure 16: Gene expression of myogenin, myostatin and myo D during C2C12 muscle differentiation.

*Quantitative real time RT PCR was used to determine the relative gene expression of muscle differentiation markers, myostatin (a) and myogenin (b) and MyoD (c) during differentiation of C2C12 myoblasts (day zero) to six days. Differentiation was reflected by significant increase in expression of all three genes between days zero and day six and day three and day six. No significant change was noted between day one and day three of differentiation. The mean relative expression is shown ±SEM (*p<0.05 n=3).*

10.2 Characterisation of Vitamin D effects on C2C12

One of the aims of this project was to confirm the expression the *muVDR, muCyp27B1* and *muCyp24A1* during differentiation of C2C12 myoblast to myofibres. RNA was

extracted from cells at the myoblast stage (day zero), day three and day six of differentiation (section 9.2.1). Subsequently, cDNA was generated and quantitative real time PCR was performed to analyse gene expression (sections 9.2.2 and 9.2.3). The *muVDR* had low levels of expression which did not change over differentiation. Similarly, *muCyp24A1* and *muCyp27B1* were also not highly expressed and their expression levels showed no significant changes over differentiation (Figure 17).

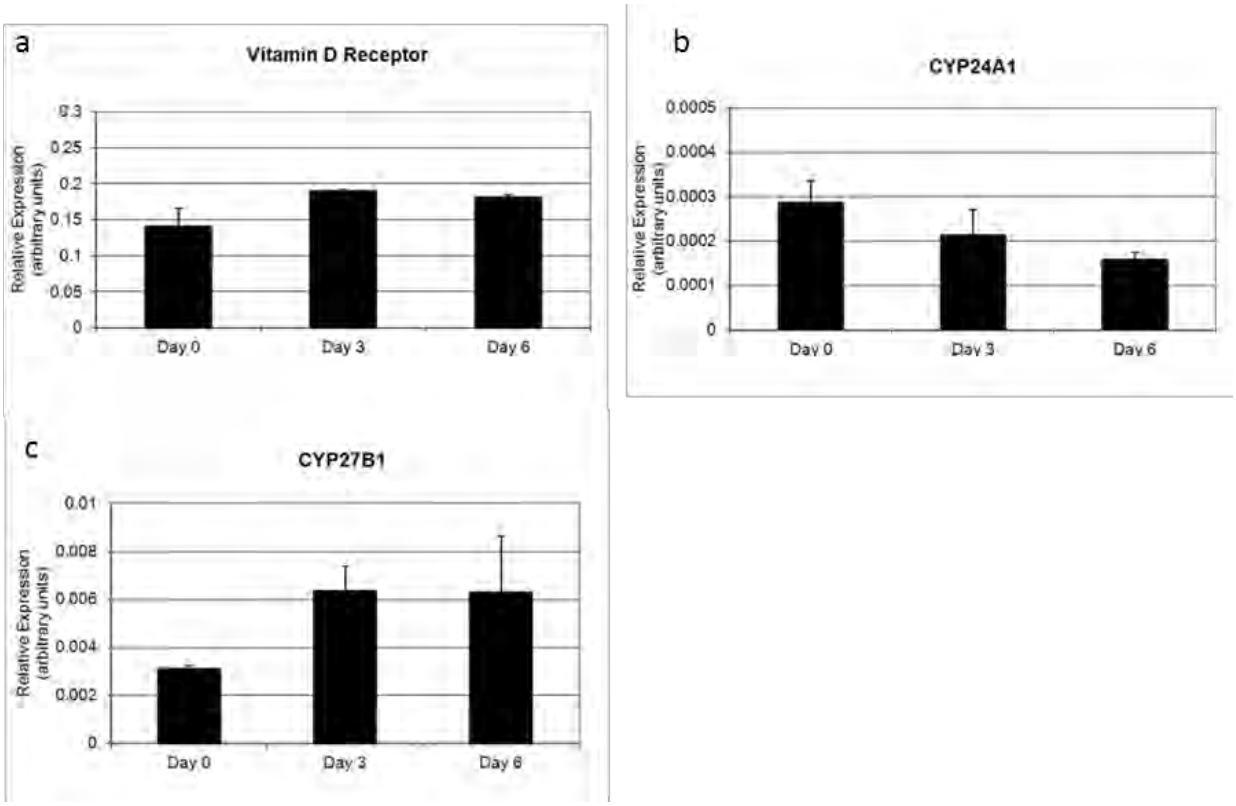

Figure 17: Gene expression of muVDR, muCyp24A1 and muCyp27B1 during C2C12 muscle differentiation.

Quantitative real time RT PCR was used to determine the relative gene expression of mouse vitamin D receptor (a), Cyp24A1 which encodes the inactivating enzyme 24-hydroxylase (b) and Cyp27B1 which encodes the activating enzyme 25-hydroxyvitamin D3-1α-hydroxylase (c). No significant difference in expression of these genes was observed during C2C12 myoblast differentiation into day six myoblasts The mean relative expression is shown ±SEM (n=3).

Given that *muVDR*, *muCyp24A1* and *muCyp27B1* showed relatively low levels of expression within the C2C12 muscle model (as determined by quantitative RT-PCR), it was important to confirm the expression of these genes was sufficient for this model to respond to vitamin D stimulation. Therefore, day six C2C12s were treated with 10nM 1α,25(OH_2)D_3 or a vehicle control containing 0.1% ethanol. After 24 hours, the RNA was extracted and cDNA was generated (sections 9.2.1 and 9.2.2). Gene expression by quantitative RT-PCR (section 9.2.3) showed that the *muVDR* and the gene responsible for the catabolism of vitamin D, *muCyp24A1* were up-regulated upon treatment with 1α,25(OH_2)D_3 (Figure 18 a and b). *muVDR* had a significant five fold up regulation when compared to the vehicle control (2.4AU ±0.08 to 11.38AU ±1.92; $p<0.05$). Similarly, *muCyp24A1* had more than 1000 fold up regulation when treated with 1α,25(OH_2)D_3 when compared to the vehicle control (0.0004AU ±9.8E-05 to 0.47±0.15; $p<0.01$). The expression of the activating enzyme *muCyp27B1* remained unchanged after treatment (Figure 18).

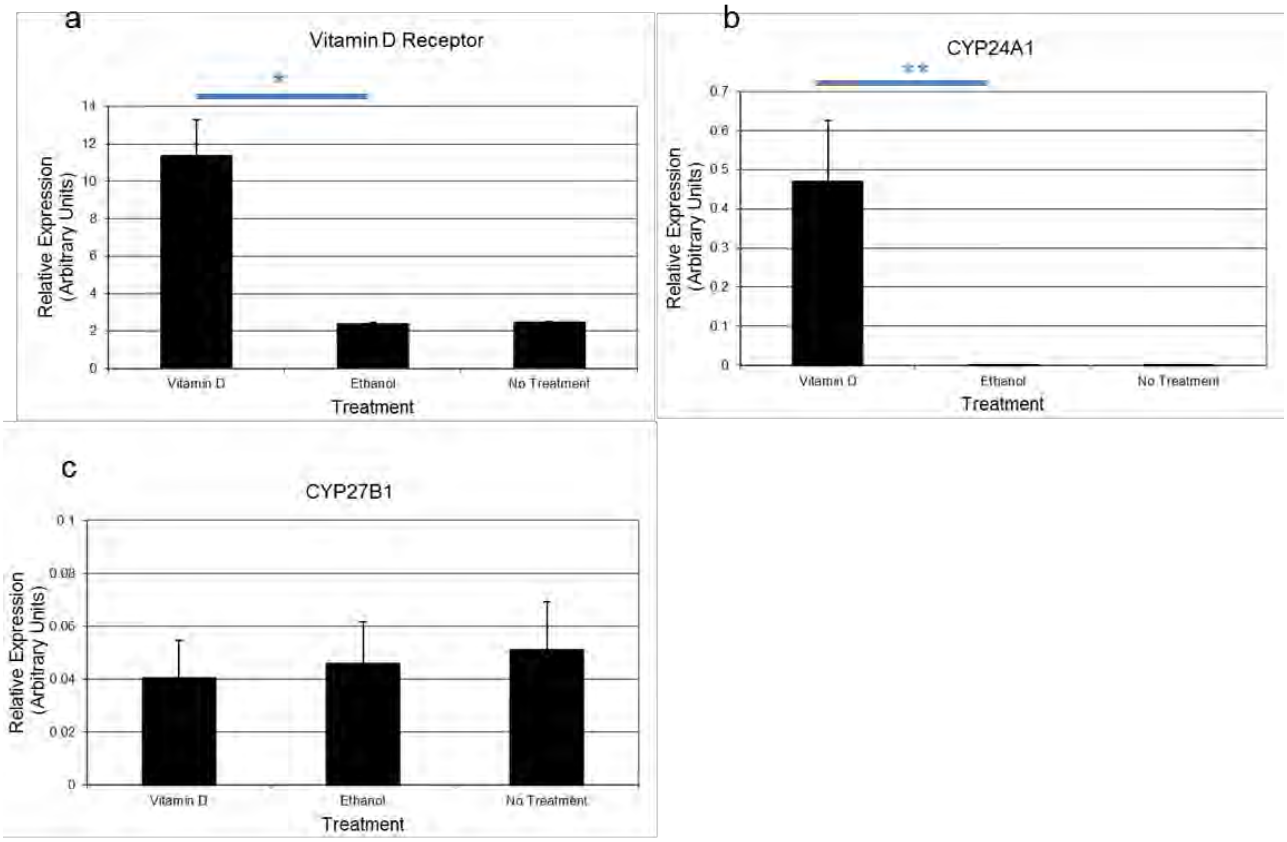

Figure 18: Gene expression of muVDR, muCyp24A1 and Cyp27B1 in response to vitamin D treatment.

Quantitative real time RT PCR was used to determine the relative gene expression of mouse vitamin D receptor (a), Cyp24A1 which encodes the inactivating enzyme 24-hydroxylase (b) and Cyp27B1 which encodes the activating enzyme 25-hydroxyvitamin D3-1α-hydroxylase (c) in day six differentiated myofibres after 24 hour treatment with 10nM 1α,25(OH$_2$)D$_3$. Both the muVDR and muCyp24A1 were significantly up regulated five fold and 1000 fold, respectively, when compared to the 0.1% ethanol treated control. muCyp27B1 expression remains unchanged after treatment. The mean relative expression is shown ±SEM (p<0.05. ** p<0.01. n=3).*

10.3 Effects of inflammatory cytokines on C2C12 myofibres

10.3.1 TNFα, IL-6 and IL-1β treatment of C2C12 myofibres

The primary aim of this project was to determine if inflammatory related muscle atrophy is a directly mediated through vitamin D actions or metabolism. To test this hypothesis, day six differentiated C2C12 were treated with key inflammatory cytokines, rmTNFα (10ng/mL), rmIL-6 (25ng/mL) and rhIL-1β (10ng/mL) for 24 hours (section 9.1.2). After treatment the expression of *muVDR*, *muCyp24A1* and *muCyp27B1* was analysed using quantitative RT-PCR (section 9.2.3).

Visual inspection of the cells after the 24 hour treatment showed no obvious changes in the morphology and formation of the C2C12 myofibres when compared to untreated controls (Figure 19).

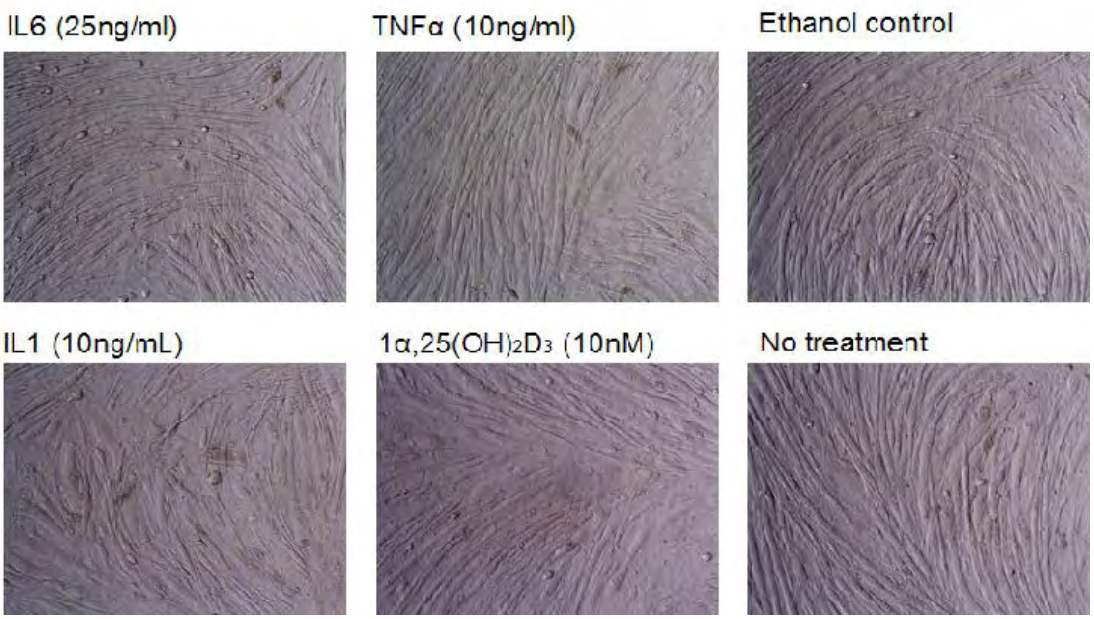

Figure 19: Cell morphology in day six treated C2C12 after treatment.

Day six differentiated C2C12 cells were treated with the pro-inflammatory cytokines rmIL-6 (25ng/mL), rmTNFα (10ng/mL) or rhIL-1β (10ng/mL). Cells were also treated with 10mM 1α,25(OH$_2$)D$_3$ and a vehicle control (ethanol). Visual inspection of the cells after 24 hours with light microscopy showed no changes in fibre morphology.

After 24 hours treatment, RNA was extracted (section 9.2.1), cDNA was generated (section 9.2.2) and quantitative RT PCR (section 9.2.3) was used to establish if inflammatory cytokines had a direct effect on expression of the vitamin D metabolism genes or receptor. No significant changes were observed in the *muVDR*, or its metabolism *muCyp27B1* or *muCyp24A1* (Figure 20).

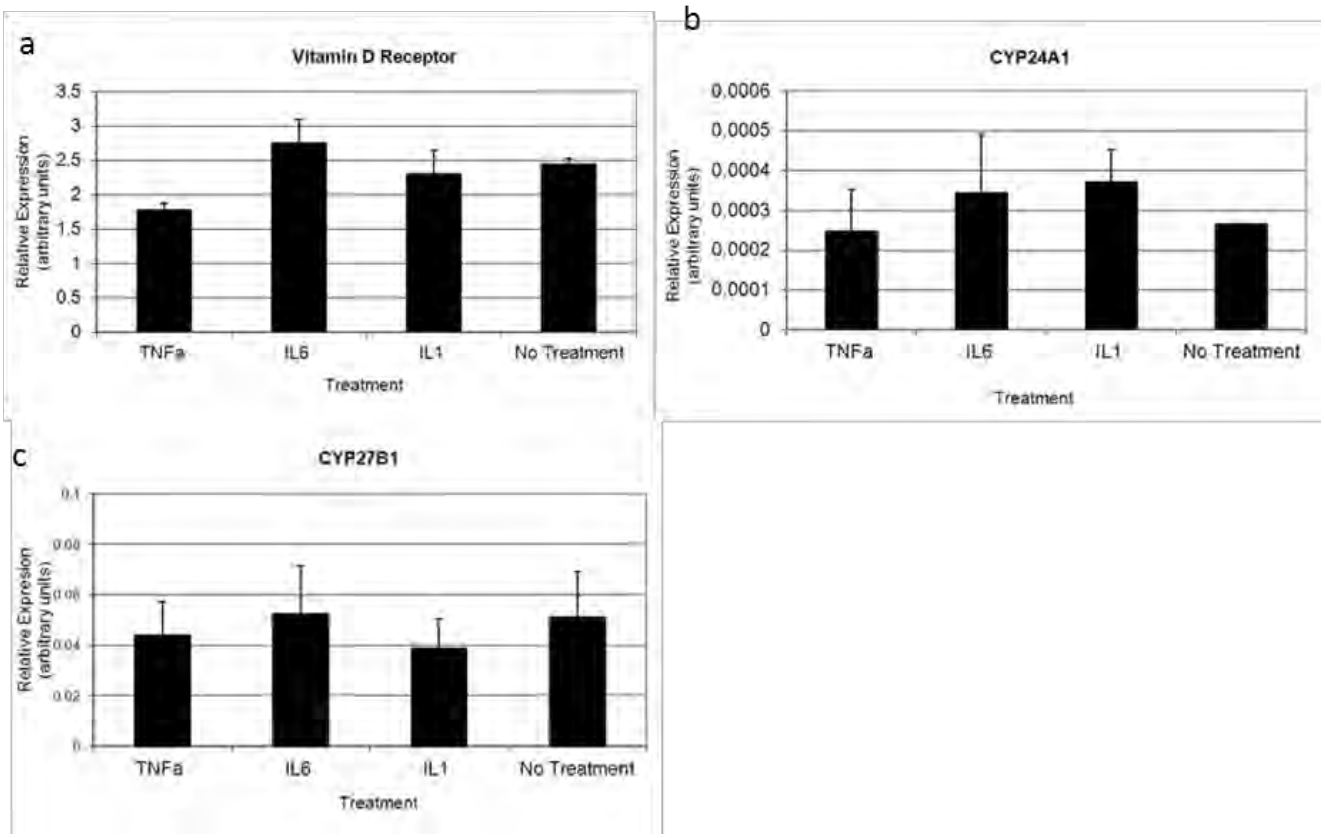

Figure 20: Gene expression of muVDR, muCyp24A1 and Cyp24B1 in response to inflammatory cytokine treatment.

Quantitative real time RT PCR was used to determine the relative gene expression of mouse vitamin D receptor (a), Cyp24A1 which encodes the inactivating enzyme 24-hydroxylase (b) and Cyp27B1 which encodes the activating enzyme 25-hydroxyvitamin D3-1α-hydroxylase (c) in day six differentiated myofibres after 24 hours after treatment with rmTNFα (10ng/ml), rmIL-6 (25ng/ml) and rmIL-1β (10ng/ml). No significant changes were observed between treated and the untreated controls. The mean relative expression is shown ±SEM (n=3).

To ensure muscle atrophy was being induced, quantitative RT PCR (section 9.2.3) was also used to examine key atrophy markers *muMAFbx* and *muMuRF1*. As previously mentioned, these enzymes are key regulators of the protein degradation through the E3 ubiquitin ligase pathway during muscle atrophy. Dexamethasone acts primarily as a

catabolic factor and therefore was used as a positive control to determine if muscle atrophy was being induced. Gene expression confirmed that 10nM dexamethasone was capable of inducing muscle atrophy within 24 hours as represented by a significant increase in *muMAFbx* when compared to untreated controls (8.7AU ±3.14 to 39.1AU ±5.36; $p<0.05$). An increase of *muRF1* was observed with dexamethasone treatment, however this was not significant. Additionally, treatment with 10ng/mL rmTNFα, 25ng/mL rmIL-6 or 10ng/ml rhIL-1β did not increase expression of muscle atrophy markers when compared with untreated cells (Figure 21).

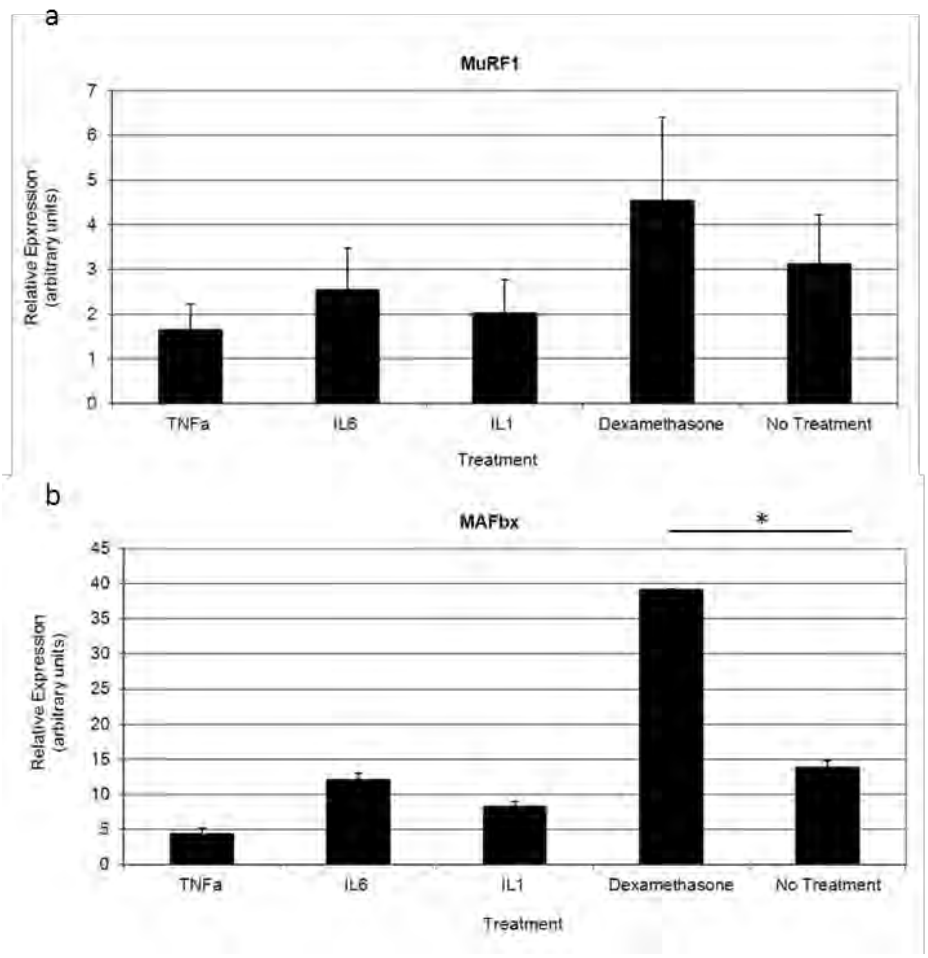

Figure 21: Gene expression of muMAFbx and muMuRF1 after 24 hour treatment with inflammatory cytokines.

*Quantitative real time RT PCR was used to determine the relative gene expression of skeletal muscle atrophy markers muMuRF1 (a) and muMAFbx (b) in day six differentiated myofibres after 24 hours after treatment with rmTNFα (10ng/mL), rmIL-6 (25ng/mL) and rhIL-1β (10ng/mL). No significant changes were observed between the cytokine treated and untreated controls. The catabolic factor dexamethasone (10nM), was used to show induction of atrophy through increased mRNA production of these genes. Treatment with dexamethasone caused significant up regulation of muMAFbx gene. The mean relative expression is shown ±SEM (*p<0.05; n=2).*

10.3.2 Differentiation of C2C12 myofibres in preconditioned media

Although the major inflammatory cytokines (i.e. rmTNFα, rmIL-6 or rhIL-1β) did not affect gene mRNA levels of *muVDR*, *muCyp24A1* or *muCyp27B1*, other factors relevant to the RA synovial milieu may have an effect on this pathway. To identify if other factors were mediating the regulation of these genes, C2C12s were differentiated in preconditioned media (section 9.1.3). This media contained cytokines and growth factors secreted from human RA synovial cells previously treated with TNFα or dexamethasone. After six days of differentiation in the presence of preconditioned media, mRNA for gene of the vitamin D pathway was assessed using quantitative real time RT PCR (section 9.2.3). Differentiation of C2C12s in the presence of pre-conditioned media from synovial fibroblasts exposed to pro- or anti-inflammatory factors showed no significant changes in the *muVDR* expression or the expression of vitamin D metabolism genes *Cyp27B1* or *Cyp24A1* (Figure 22).

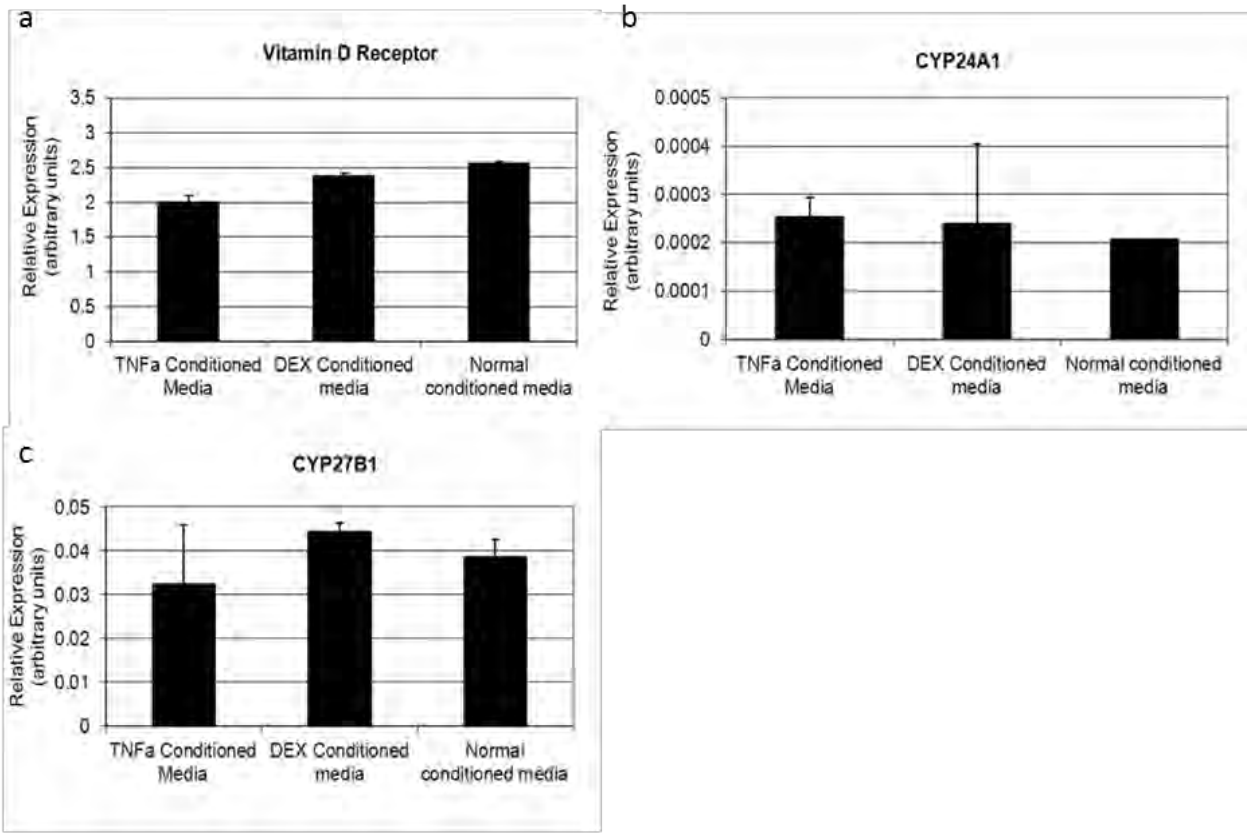

Figure 22: Gene expression of muVDR, muCyp24A1 and Cyp24B1 in response to differentiation in the presence of preconditioned media.

Quantitative real time RT PCR was used to determine the relative gene expression of mouse vitamin D receptor (a), Cyp24A1 which encodes the vitamin D catabolising enzyme 24-hydroxylase (b) and Cyp27B1 which encodes the activating enzyme 25-hydroxyvitamin D3-1α-hydroxylase after six days of differentiation (c). Myoblasts were differentiated in preconditioned media from human RA synovial fibroblasts treated with TNFα, dexamethasone (DEX), or had remained untreated. No significant changes were observed between the different treatments. The mean relative expression is shown ±SEM (n=2).

To determine if the cytokine or dexamethasone-conditioned media were having an effect on muscle differentiation, gene expression of myogenic regulatory markers were assessed from day six myofibres (section 9.1.3). The results showed that there was no significant

change in the expression of myostatin or myogenin in cells treated with preconditioned media when compared to cells differentiated in untreated conditioned media (Figure 23).

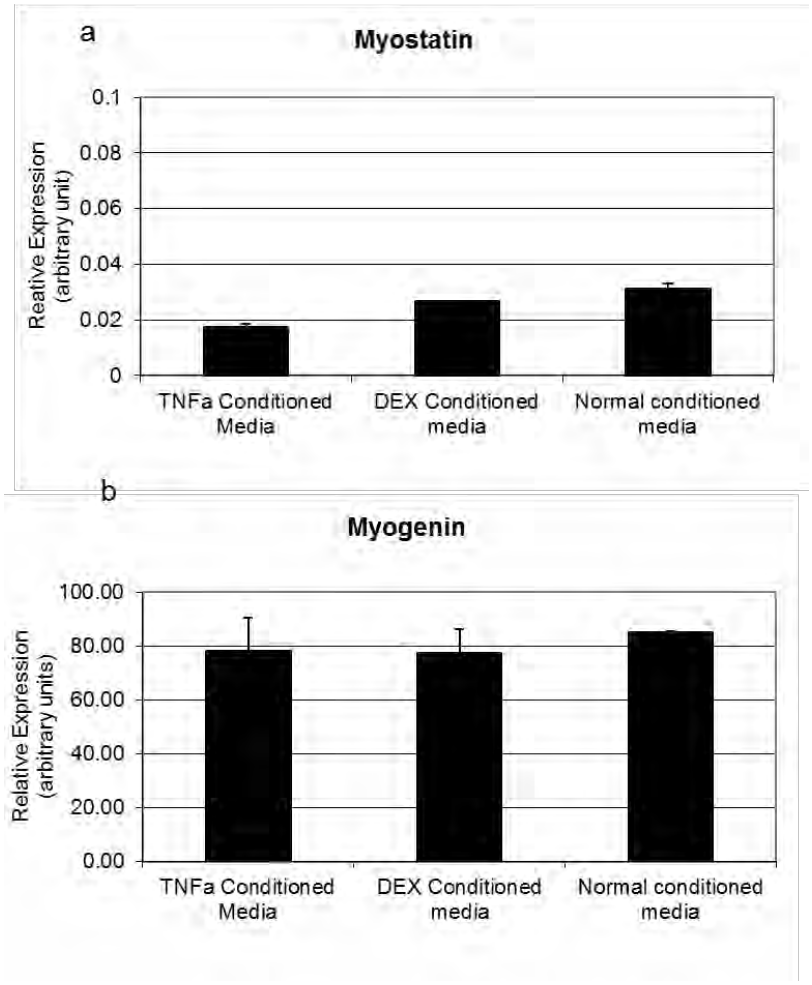

Figure 23: Gene expression of myostatin and myogenin in response to differentiation in the presence of preconditioned media.

Quantitative real time RT PCR was used to determine the relative gene expression of muscle differentiation markers, myostatin (a) and myogenin (b) after six days of differentiation. Myoblasts were differentiated in pre conditioned media from human RA synovial fibroblasts treated with TNFα, dexamethasone (DEX), or fibroblasts that remained untreated. No significant changes were observed between the different treatments. The mean relative expression is shown ±SEM (n=2).

In order to examine if muscle atrophy was being induced by the presence of other agents in the preconditioned media, the expression of the ubiquitin ligase proteins *muMuRF1* and *muMAFbx* were observed. After six days of differentiation in the preconditioned media, RNA was extracted (section 9.2.1), cDNA was generated (section 9.2.2) and quantitative real time RT-PCR was performed (section 9.2.3). *muMuRF1* showed no change between cells treated with conditioned media induced with TNFα or dexamethasone and the normal conditioned media. There was a slight up regulation of *muMAFbx* with the conditioned media from TNFα treated synovial fibroblasts, however, this change was not significant (Figure 24).

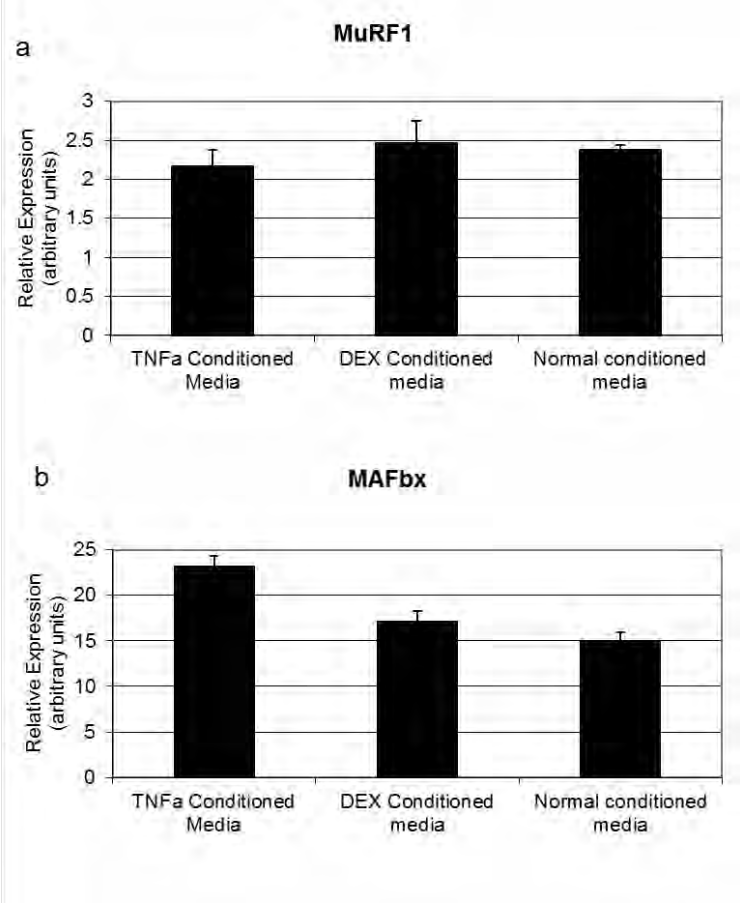

Figure 24: Gene expression of MuRF1 and MAFbx in response to differentiation in the presence of preconditioned media.

Quantitative Real time RT PCR was used to determine the relative gene expression of skeletal muscle atrophy markers muMuRF1 (a) and muMAFbx (b) after six days of differentiation. Myoblasts were differentiated in pre conditioned media from human RA synovial fibroblasts treated with TNFα, dexamethasone (DEX), or had remained untreated. No significant changes were observed between the different treatments. The mean relative expression is shown ±SEM (n=2).

10.4 Vitamin D effects on muscle differentiation

It has been suggested that vitamin D has a positive effect on skeletal muscle differentiation. In order to determine the actions of vitamin D on C2C12 muscle cells,

myoblasts underwent differentiation in the presence of either 1nM, 10nM or 100nM of $1,25(OH)_2D_3$ (section 9.1.4) . Cells also were differentiated in the absence $1,25(OH)_2D_3$ or in 0.1% ethanol as a vehicle control. Cells were harvested at day one, three and six for gene expression analysis by quantitative real time RT PCR (section 9.2.3).

To investigate the effects of vitamin D on differentiation or proliferation, expression of key myogenic regulatory factors which have key roles in myoblast differentiation and skeletal muscle development were measured. $1,25(OH)_2D_3$ had no significant effects on the expression of MyoD, myogenin or myostatin at any concentration during differentiation of myoblast to myofibres (Figure 25).

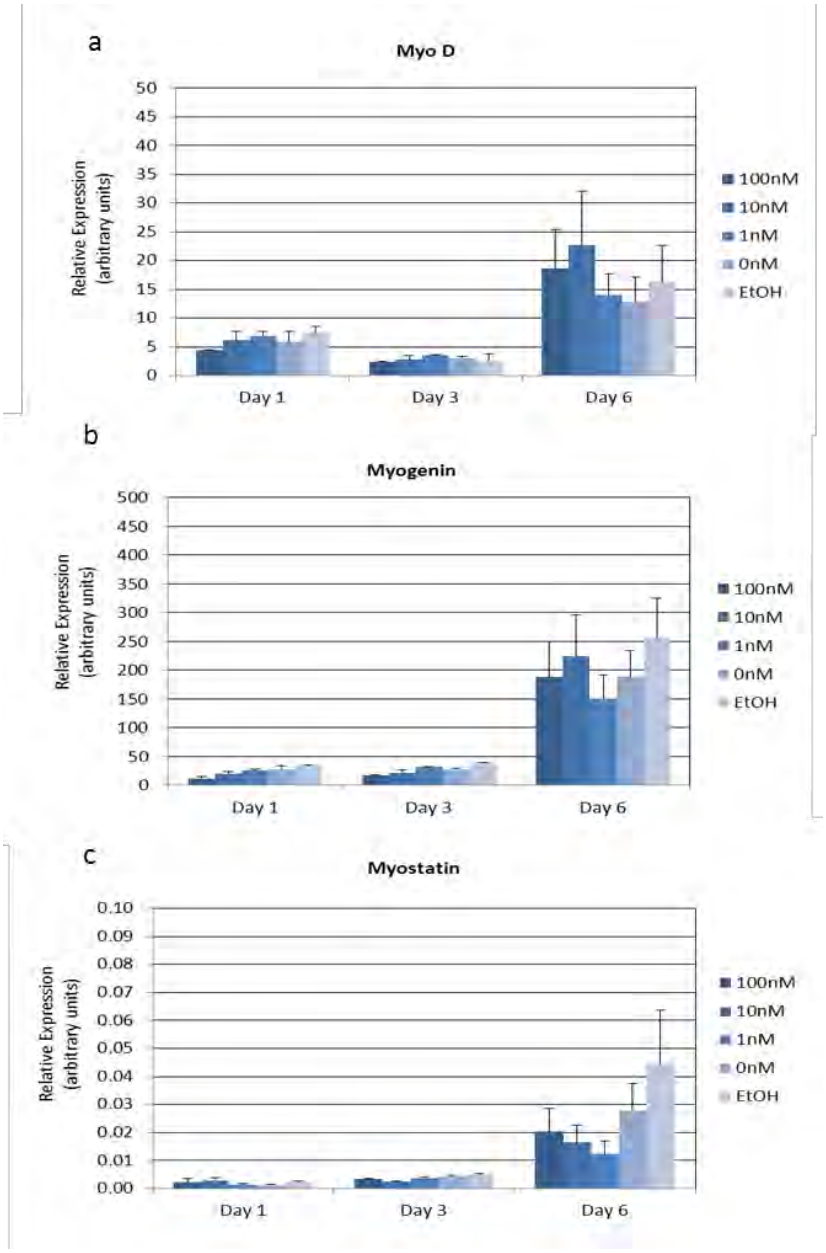

Figure 25: Gene expression of myo D, myogenin and myostatin in response to differentiation of C2C12 myoblasts in the presence of vitamin D.

Quantitative real time RT PCR was used to determine the relative gene expression of muscle differentiation markers, Myo D (a), myogenin (b) and myostatin (c) during differentiation of myoblasts to day six myofibres. Myoblasts were differentiated in the presence of 100nM, 10nM or 1nM of 1,25(OH)$_2$D$_3$ and cells were harvested on day one, day three and day six. No significant changes were observed between the different treatments. The mean relative expression is shown ±SEM (n=2).

11 DISCUSSION

11.1 Vitamin D actions and metabolism in C2C12 cells

We hypothesised that inflammatory related skeletal muscle atrophy is a direct result of changes in vitamin D activity or its metabolism. However, we failed to find support for this hypothesis through a variety of experiments using murine C2C12 myofibres. We were able to confirm that the C2C12 muscle model expressed the *muVDR*, *muCyp27B1* and *muCyp24A1* in relatively low levels. It was also confirmed that the level of expression did not show significant changes during differentiation. This contradicts other reported models where the VDR increases expression during differentiation from myoblasts to myofibres (Simpson et al., 1985).

As highlighted, $1\alpha,25(OH_2)D_3$ is the active metabolite of vitamin D and it exerts its action through the nuclear VDR by regulating transcriptional responses within the cell. However, the precise effect of vitamin D on skeletal muscle remains controversial. Despite the relatively low levels of expression observed in this study, day six differentiated myofibres were able to respond to 10nM $1\alpha,25(OH_2)D_3$. With a 24 hour treatment there was a significant increase in expression of *muVDR* ($p<0.05$) and the $1\alpha,25(OH_2)D_3$ inactivating *muCyp24A1* gene ($p<0.01$) when compared to the vehicle treated controls. The up regulation of these genes is a well established auto-regulatory mechanism of vitamin D action in other tissues. Furthermore, $1\alpha,25(OH_2)D_3$ is also capable of transcriptional repression of *Cyp27B1* through a negative regulating VDRE within its promoter (Deeb et al., 2007). However, in this study, repression of

muCyp27B1 was not observed in C2C12 myofibres after 24 hour treatment with $1\alpha,25(OH_2)D_3$.

11.2 Inflammatory cytokines effects of vitamin D metabolism

Inflammatory autoimmune conditions such as RA, are associated with decreased levels of vitamin D, as well as an increased presence of pro-inflammatory cytokines. Cytokines such as TNFα, IL-6 and IL-1β are known to promote skeletal muscle loss in inflammatory diseases like RA (Argiles and Lopez-Soriano, 1999). Furthermore, vitamin D deficiency also results in muscle wasting (Pfeifer et al., 2002). Therefore, it was hypothesised that inflammation related muscle loss is due to effects on vitamin D action through the VDR or vitamin D metabolism in muscle cells.

To determine if inflammatory related muscle wasting was from direct changes in vitamin D action or metabolism, expression of the key vitamin D genes were observed following a 24 hour treatment with inflammatory cytokines. Neither rmTNFα, rmIL-6 nor rhIL-1β had an effect on the *muVDR*, the vitamin D activating enzyme *muCyp27B1*, or its inactivating enzyme *muCyp24A1*.

Although rmTNFα, rmIL-6 and rhIL-1β were shown not to directly influence the vitamin D metabolism genes, it was not possible to rule out a combination of these factors or that other growth factors or cytokines may have an effect. Therefore, cells were differentiated for six days in the presence of serum extracted from human RA synovial fibroblasts

treated with TNFα or dexamethasone. After six days, expression of *muVDR*, *muCyp27B1*, and *muCyp24A1* remained unchanged compared to the controls. This disproves the original hypothesis and suggests that inflammatory cytokines are not directly regulating vitamin D action or metabolism in skeletal muscle.

11.3 Modelling inflammatory related muscle atrophy in C2C12 myofibres.

Inflammatory cytokines, specifically TNFα, IL-6 and IL-1β are capable of inducing muscle atrophy. To confirm whether muscle atrophy was being induced in our C2C12 model, gene expression of atrophy markers *muMuRF1* and *muMAFbx* were analysed. *muMuRF1* and *muMAFbx* are E3 ligase of the ubiquitin proteasome pathway and their mRNA expression is known to increase during muscle atrophy (Sandri, 2008).

24 hour treatment with 10ng/mL rmTNFα, 10ng/mL rmIL-6 or 25ng/mL rhIL-1β was not sufficient to regulate the mRNA level of these key atrophy markers within day six differentiated myofibres. Treatment with the catabolic factor 10nM dexamethasone did confirm that 24 hours was a sufficient length of time to induce significant up regulation of *muMAFbx*. Similarly, when cells were treated with serum conditioned media over six days of differentiation, there was no change in expression of the E3 ubiquitin ligase gene expression. This suggests we were unable to accurately model skeletal muscle atrophy in C2C12s.

The possibility that muscle atrophy in C2C12 myofibres can be induced by higher concentrations of inflammatory cytokines cannot be excluded. However, this study used concentrations based on physiological levels for chronic inflammatory disease, as well as concentrations observed in previous studies on C2C12 cells (Al-Khalili et al., 2006, Li et al., 2009, Li et al., 2005). The concentrations of pro-inflammatory cytokines used in this study did not regulate mRNA levels of key myogenic factors, but skeletal muscle atrophy can also be assessed by other changes in the cell, such as changes in muscle fibre size (Sultan et al., 2006) or down regulation of muscle growth signalling pathways (Kandarian and Jackman, 2006). However, none of these other muscle atrophy characteristics were investigated and consequently represent a limitation of the current study.

Interestingly, IL-6 can directly induce skeletal muscle atrophy through activation of JAK/STAT signalling pathway causing subsequent down regulation of intracellular signalling (Haddad et al., 2005). This study also confirmed that mRNA for E3 ubiquitin protein liagases *MAFbx* and *MuRF1* did not change in response to IL-6 treatment (Haddad et al., 2005). This supports the results in this current study. As IL-6 muscle atrophy is not mediated via the ubiquitin ligase pathway, and therefore no change in the expression of the protein ligases would be expected.

Previous studies have suggested that examination of gene expression after 24 hours of treatment may mask the up regulation of the ubiquitin protein liagases. 6ng/mL TNFα treatment of day four differentiated C2C12 mytubes was sufficient to induce significant up regulation of *muMAFbx* within two hours (Li et al., 2005). Additionally, after six

hours post treatment, *muMAFbx* expression levels returned to control levels and remained unchanged from 12 and 24 hours. This is consistent with the results observed in this study, as there was no increase from control level after 24 hours of treatment. However, it can not be concluded that there was significant up regulation of *muMAFbx* at two hours post treatment. Therefore a limitation of this current study that needs to be considered is only gene expression at 24 hours after treatment was investigated.

It must also be noted that this study was limited to investigating mouse muscle, not human. We failed to find evidence to suggest that inflammatory cytokines influence vitamin D action or its metabolism in murine C2C12 myofibres. However, this may not be a true representation of what occurs in human patients. *In vitro* studies investigating the influence of inflammatory agents on muscle are commonly performed in C2C12, however, the results are often inconsistent (Petersen et al., 2009). Therefore, it is proposed that human primary cultures will provide confirmation that results observed in this study can be translated to human muscle atrophy cases.

11.4 Indirect effects of Vitamin D on inflammatory related muscle atrophy

In contrast to the hypothesis, this current study demonstrated that inflammation-related muscle atrophy does not result from changes in vitamin D action through the VDR or its metabolism via 24-OHase or 25-OHase. There is evidence to suggest vitamin D may have indirect effects which can be beneficial to inflammatory related skeletal muscle

atrophy. Briefly, vitamin D has been observed to have direct effects on cells of the immune system and consequently down regulate their immune response. Vitamin D is capable of inhibiting secretion of pro-inflammatory macrophage derived cytokines, such as TNFα, IL-1β, IL-6 and IL-12 all of which are elevated in RA patients (Wen and Baker, 2011). In addition, vitamin D is associated with down regulating signalling pathways induced during inflammatory related muscle loss (Bikle, 2009). Therefore, through these suggested indirect mechanisms, it is possible that vitamin D may help decrease muscle atrophy caused by inflammatory cytokines.

11.5 Vitamin D and muscle differentiation

Vitamin D supplementation may be used as a preventative measure for patients who are high risk of acquiring vitamin D deficiency and subsequent muscle atrophy. Despite the precise mechanism of vitamin D action on muscle being unknown, some clinical and experimental studies have suggested it has important roles in muscle function and development including effects on proliferation and differentiation (Ceglia, 2008). Treatment of C2C12s with 10nM of $1\alpha,25(OH_2)D_3$ for 24 hours, showed a marked increase in expression of the VDR confirming that the cells are responsive to this steroid. However, differentiating myoblasts in the presence of 1nM, 10nM or 100nM $1\alpha,25(OH_2)D_3$ had no influence in the formation of myofibres. During myogenesis, myoblasts stop proliferation and fuse into myofibres. A study by Stio et. al. (2002) confirmed that 1nM of $1\alpha,25(OH_2)D_3$ was ineffective in inhibiting cell proliferation of myoblasts or influencing their differentiation. This study also indicated that vitamin D

analogues were able to promote myogenesis in C2C12 cells, and therefore concluded that perhaps higher concentrations of $1\alpha,25(OH_2)D_3$ were required to observe this effect. However, this current study suggests that higher concentrations of $1\alpha,25(OH_2)D_3$ are also unable to influence myoblast proliferation or differentiation.

12 CONCLUSIONS AND FUTURE DIRECTIONS

RA is a complicated disease which can be influenced by both genetic and environmental factors. Currently, the treatment of RA requires a multiple approach using medications, regular follow ups, physiotherapy, joint protection and self management. Patients often suffer skeletal muscle atrophy from whole systemic inflammation which inturn leads to general muscle weakness, impairment of normal activities and an increase in mortality. This project aimed to investigate muscle atrophy caused by inflammation and whether it results through direct changes in vitamin D action or metabolism. We were unable to find any support for this hypothesis through a variety of experiments and therefore conclude that inflammatory related muscle loss is not mediated through vitamin D. We found that pro-inflammatory cytokines had no effect on the expression of the *muVDR* or vitamin D key metabolism genes *muCyp27Al* or *muCyp24B1*. As this study was limited to C2C12 mouse cell line, further *in vitro* studies with human primary cultures would be recommended to confirm the findings from this study.

The results observed in this study can be directly translated to clinical management of patients and it would not be recommended that vitamin D be the sole treatment of inflammatory related muscle loss. However, there is evidence to suggest that vitamin D can inhibit inflammatory components as well as down regulate their signalling pathway. Therefore vitamin D may have indirect benefits on atrophying muscle cells through inhibiting inflammatory actions.

Current reports on the actions of vitamin D in muscle are somewhat contradictory. Further research into the effects and underlying molecular action of vitamin D on skeletal muscle is required. Specifically, what genes are regulated through activation of the VDR will give insight into how vitamin D influences skeletal muscle. Clinical trials investigating the relationship between vitamin D and muscle have also given conflicting results. Additionally, there is an absence of randomised controlled trials examining vitamin D supplementation in diseases where vitamin D deficiency is frequent. Further well-designed clinical trials observing the effects of vitamin D on muscle are required. In addition, studies are needed to determine the optimal level of vitamin D in the blood to achieve maximal benefit to patients.

Skeletal muscle atrophy is common in chronic inflammatory diseases such as RA. However, currently there is no effective pharmacological treatment option for it regardless of its origin. Loss of muscle mass results in muscle weakness, an increase risk of falls and fractures and can increase the mortality and morbidity associated with the initial disease. Therefore, determining the precise pathological mechanisms promoting inflammatory related muscle atrophy remains of high clinical importance.

REFERENCE

Ahmad, M., Haque, M. F., Ahmad, W., Abbas, H., Haque, S., Krakow, D., Rimoin, D. L., Lachman, R. S. & Cohn, D. H. (1998) Distinct, autosomal recessive form of spondyloepimetaphyseal dysplasia segregating in an inbred Pakistani kindred. *Am J Med Genet,* 78**,** 468-473.

Al-Khalili, L., Bouzakri, K., Glund, S., Lonnqvist, F., Koistinen, H. A. & Krook, A. (2006) Signaling specificity of interleukin-6 action on glucose and lipid metabolism in skeletal muscle. *Mol Endocrinol,* 20**,** 3364-3375.

Argiles, J. M. & Lopez-Soriano, F. J. (1999) The role of cytokines in cancer cachexia. *Med Res Rev,* 19**,** 223-248.

Auchus, R. J. (2004) Overview of dehydroepiandrosterone biosynthesis. *Semin Reprod Med,* 22**,** 281-288.

Baltgalvis, K. A., Berger, F. G., Pena, M. M., Davis, J. M., White, J. P. & Carson, J. A. (2009) Muscle wasting and interleukin-6-induced atrogin-I expression in the cachectic Apc (Min/+) mouse. *Pflugers Arch,* 457**,** 989-1001.

Besset, S., Vincourt, J. B., Amalric, F. & Girard, J. P. (2000) Nuclear localization of PAPS synthetase 1: a sulfate activation pathway in the nucleus of eukaryotic cells. *Faseb J,* 14**,** 345-354.

Bikle, D. (2009) Nonclassic actions of vitamin D. *J Clin Endocrinol Metab,* 94**,** 26-34.

Bischoff-Ferrari, H. A., Dawson-Hughes, B., Staehelin, H. B., Orav, J. E., Stuck, A. E., Theiler, R., Wong, J. B., Egli, A., Kiel, D. P. & Henschkowski, J. (2009) Fall prevention with supplemental and active forms of vitamin D: a meta-analysis of randomised controlled trials. *Bmj,* 339**,** b3692.

Bischoff, H. A., Borchers, M., Gudat, F., Duermueller, U., Theiler, R., Stahelin, H. B. & Dick, W. (2001) In situ detection of 1,25-dihydroxyvitamin D3 receptor in human skeletal muscle tissue. *Histochem J,* 33**,** 19-24.

Bischoff, H. A., Stahelin, H. B., Dick, W., Akos, R., Knecht, M., Salis, C., Nebiker, M., Theiler, R., Pfeifer, M., Begerow, B., Lew, R. A. & Conzelmann, M. (2003) Effects of vitamin D and calcium supplementation on falls: a randomized controlled trial. *J Bone Miner Res,* 18**,** 343-351.

Blanchard, R. L., Freimuth, R. R., Buck, J., Weinshilboum, R. M. & Coughtrie, M. W. (2004) A proposed nomenclature system for the cytosolic sulfotransferase (SULT) superfamily. *Pharmacogenetics,* 14**,** 199-211.

Bodine, S. C., Latres, E., Baumhueter, S., Lai, V. K., Nunez, L., Clarke, B. A.,

Poueymirou, W. T., Panaro, F. J., Na, E., Dharmarajan, K., Pan, Z. Q., Valenzuela, D. M., Dechiara, T. M., Stitt, T. N., Yancopoulos, G. D. & Glass, D. J. (2001) Identification of ubiquitin ligases required for skeletal muscle atrophy. *Science,* 294**,** 1704-1708.

Ceglia, L. (2008) Vitamin D and skeletal muscle tissue and function. *Mol Aspects Med,* 29**,** 407-414.

Chung, B. C., Picado-Leonard, J., Haniu, M., Bienkowski, M., Hall, P. F., Shively, J. E. & Miller, W. L. (1987) Cytochrome P450c17 (steroid 17 alpha-hydroxylase/17,20 lyase): cloning of human adrenal and testis cDNAs indicates the same gene is expressed in both tissues. *Proc Natl Acad Sci U S A,* 84**,** 407-411.

Cooney, R. N., Maish, G. O., 3rd, Gilpin, T., Shumate, M. L., Lang, C. H. & Vary, T. C. (1999) Mechanism of IL-1 induced inhibition of protein synthesis in skeletal muscle. *Shock,* 11**,** 235-241.

Cutler, G. B., Jr., Glenn, M., Bush, M., Hodgen, G. D., Graham, C. E. & Loriaux, D. L. (1978) Adrenarche: a survey of rodents, domestic animals, and primates. *Endocrinology,* 103**,** 2112-2118.

Cutolo, M., Otsa, K., Yprus, M. & Seriolo, B. (2007) Vitamin D and rheumatoid arthritis: comment on the letter by Nielen et al. *Arthritis Rheum,* 56**,** 1719-1720.

Deeb, K. K., Trump, D. L. & Johnson, C. S. (2007) Vitamin D signalling pathways in cancer: potential for anticancer therapeutics. *Nat Rev Cancer,* 7**,** 684-700.

Drittanti, L., De Boland, A. R. & Boland, R. (1989) Modulation of DNA synthesis in cultured muscle cells by 1,25-dihydroxyvitamin D-3. *Biochim Biophys Acta,* 1014**,** 112-119.

Ebeling, P. & Koivisto, V. A. (1994) Physiological importance of dehydroepiandrosterone. *Lancet,* 343**,** 1479-1481.

Endo, I., Inoue, D., Mitsui, T., Umaki, Y., Akaike, M., Yoshizawa, T., Kato, S. & Matsumoto, T. (2003) Deletion of vitamin D receptor gene in mice results in abnormal skeletal muscle development with deregulated expression of myoregulatory transcription factors. *Endocrinology,* 144**,** 5138-5144.

Faiyaz Ul Haque, M., King, L. M., Krakow, D., Cantor, R. M., Rusiniak, M. E., Swank, R. T., Superti-Furga, A., Haque, S., Abbas, H., Ahmad, W., Ahmad, M. & Cohn, D. H. (1998) Mutations in orthologous genes in human spondyloepimetaphyseal dysplasia and the brachymorphic mouse. *Nat Genet,* 20**,** 157-162.

Falany, C. N. (1997) Enzymology of human cytosolic sulfotransferases. *Faseb J,* 11**,** 206-216.

Falany, C. N., Xie, X., Wang, J., Ferrer, J. & Falany, J. L. (2000) Molecular cloning and expression of novel sulphotransferase-like cDNAs from human and rat brain. *Biochem J,*

346 Pt 3**,** 857-864.

Firestein, G. S. (2003) Evolving concepts of rheumatoid arthritis. *Nature,* 423**,** 356-361.

Flicker, L., Macinnis, R. J., Stein, M. S., Scherer, S. C., Mead, K. E., Nowson, C. A., Thomas, J., Lowndes, C., Hopper, J. L. & Wark, J. D. (2005) Should older people in residential care receive vitamin D to prevent falls? Results of a randomized trial. *J Am Geriatr Soc,* 53**,** 1881-1888.

Fuda, H., Shimizu, C., Lee, Y. C., Akita, H. & Strott, C. A. (2002) Characterization and expression of human bifunctional 3'-phosphoadenosine 5'-phosphosulphate synthase isoforms. *Biochem J,* 365**,** 497-504.

Fujita, K., Nagata, K., Ozawa, S., Sasano, H. & Yamazoe, Y. (1997) Molecular cloning and characterization of rat ST1B1 and human ST1B2 cDNAs, encoding thyroid hormone sulfotransferases. *J Biochem,* 122**,** 1052-1061.

Gamage, N., Barnett, A., Hempel, N., Duggleby, R. G., Windmill, K. F., Martin, J. L. & Mcmanus, M. E. (2006) Human sulfotransferases and their role in chemical metabolism. *Toxicol Sci,* 90**,** 5-22.

Garcia-Martinez, C., Lopez-Soriano, F. J. & Argiles, J. M. (1993) Acute treatment with tumour necrosis factor-alpha induces changes in protein metabolism in rat skeletal muscle. *Mol Cell Biochem,* 125**,** 11-18.

Glass, D. J. (2003) Signalling pathways that mediate skeletal muscle hypertrophy and atrophy. *Nat Cell Biol,* 5**,** 87-90.

Grum, D., Van Den Boom, J., Neumann, D., Matena, A., Link, N. M. & Mueller, J. W. (2010) A heterodimer of human 3'-phospho-adenosine-5'-phosphosulphate (PAPS) synthases is a new sulphate activating complex. *Biochem Biophys Res Commun,* 395**,** 420-425.

Guttridge, D. C., Mayo, M. W., Madrid, L. V., Wang, C. Y. & Baldwin, A. S., Jr. (2000) NF-kappaB-induced loss of MyoD messenger RNA: possible role in muscle decay and cachexia. *Science,* 289**,** 2363-2366.

Haddad, F., Zaldivar, F., Cooper, D. M. & Adams, G. R. (2005) IL-6-induced skeletal muscle atrophy. *J Appl Physiol,* 98**,** 911-917.

Hammer, F., Subtil, S., Lux, P., Maser-Gluth, C., Stewart, P. M., Allolio, B. & Arlt, W. (2005) No evidence for hepatic conversion of dehydroepiandrosterone (DHEA) sulfate to DHEA: in vivo and in vitro studies. *J Clin Endocrinol Metab,* 90**,** 3600-3605.

Harjes, S., Bayer, P. & Scheiding, A.J. (2005) The crystal structure of human PAPS synthetase 1 Reveals Asymmetry in Substrate Binding. *J Mol Bio,* 346, 623-635.

Hazeldine, J., Arlt, W. & Lord, J. M. (2010) Dehydroepiandrosterone as a regulator of immune cell function. *J Steroid Biochem Mol Biol,* 120**,** 127-136.

Helliwell, P. S. & Jackson, S. (1994) Relationship between weakness and muscle wasting in rheumatoid arthritis. *Ann Rheum Dis,* 53**,** 726-728.

Holick, M. F. (2007) Vitamin D deficiency. *N Engl J Med,* 357**,** 266-281.

Hu, M. C., Hsu, N. C., El Hadj, N. B., Pai, C. I., Chu, H. P., Wang, C. K. & Chung, B. C. (2002) Steroid deficiency syndromes in mice with targeted disruption of Cyp11a1. *Mol Endocrinol,* 16**,** 1943-1950.

Jackman, R. W. & Kandarian, S. C. (2004) The molecular basis of skeletal muscle atrophy. *Am J Physiol Cell Physiol,* 287**,** C834-843.

Jagoe, R. T. & Goldberg, A. L. (2001) What do we really know about the ubiquitin-proteasome pathway in muscle atrophy? *Curr Opin Clin Nutr Metab Care,* 4**,** 183-190.

Kandarian, S. C. & Jackman, R. W. (2006) Intracellular signaling during skeletal muscle atrophy. *Muscle Nerve,* 33**,** 155-165.

Kim, C. J., Lin, L., Huang, N., Quigley, C. A., Avruskin, T. W., Achermann, J. C. & Miller, W. L. (2008) Severe combined adrenal and gonadal deficiency caused by novel mutations in the cholesterol side chain cleavage enzyme, P450scc. *J Clin Endocrinol Metab,* 93**,** 696-702.

Klaassen, C. D. & Boles, J. W. (1997) Sulfation and sulfotransferases 5: the importance of 3'-phosphoadenosine 5'-phosphosulfate (PAPS) in the regulation of sulfation. *Faseb J,* 11**,** 404-418.

Kroger, H., Penttila, I. M. & Alhava, E. M. (1993) Low serum vitamin D metabolites in women with rheumatoid arthritis. *Scand J Rheumatol,* 22**,** 172-177.

Kurima, K., Singh, B. & Schwartz, N. B. (1999) Genomic organization of the mouse and human genes encoding the ATP sulfurylase/adenosine 5'-phosphosulfate kinase isoform SK2. *J Biol Chem,* 274**,** 33306-33312.

Li, W., Moylan, J. S., Chambers, M. A., Smith, J. & Reid, M. B. (2009) Interleukin-1 stimulates catabolism in C2C12 myotubes. *Am J Physiol Cell Physiol,* 297**,** C706-714.

Li, Y. P., Chen, Y., John, J., Moylan, J., Jin, B., Mann, D. L. & Reid, M. B. (2005) TNF-alpha acts via p38 MAPK to stimulate expression of the ubiquitin ligase atrogin1/MAFbx in skeletal muscle. *Faseb J,* 19**,** 362-370.

Li, Y. P., Schwartz, R. J., Waddell, I. D., Holloway, B. R. & Reid, M. B. (1998) Skeletal muscle myocytes undergo protein loss and reactive oxygen-mediated NF-kappaB

activation in response to tumor necrosis factor alpha. *Faseb J,* 12**,** 871-880.

Lips, P. (2006) Vitamin D physiology. *Prog Biophys Mol Biol,* 92**,** 4-8.

Lyle, S., Stanczak, J., Ng, K. & Schwartz, N. B. (1994) Rat chondrosarcoma ATP sulfurylase and adenosine 5'-phosphosulfate kinase reside on a single bifunctional protein. *Biochemistry,* 33**,** 5920-5925.

Matschke, V., Murphy, P., Lemmey, A. B., Maddison, P. J. & Thom, J. M. (2010) Muscle quality, architecture, and activation in cachectic patients with rheumatoid arthritis. *J Rheumatol,* 37**,** 282-284.

Mcinnes, I. B. & Schett, G. (2007) Cytokines in the pathogenesis of rheumatoid arthritis. *Nat Rev Immunol,* 7**,** 429-442.

Merlino, L. A., Curtis, J., Mikuls, T. R., Cerhan, J. R., Criswell, L. A. & Saag, K. G. (2004) Vitamin D intake is inversely associated with rheumatoid arthritis: results from the Iowa Women's Health Study. *Arthritis Rheum,* 50**,** 72-77.

Miller, W. L. & Auchus, R. J. (2010) The molecular biology, biochemistry, and physiology of human steroidogenesis and its disorders. *Endocr Rev,* 32**,** 81-151.

Nakajin, S., Shinoda, M., Haniu, M., Shively, J. E. & Hall, P. F. (1984) C21 steroid side chain cleavage enzyme from porcine adrenal microsomes. Purification and characterization of the 17 alpha-hydroxylase/C17,20-lyase cytochrome P-450. *J Biol Chem,* 259**,** 3971-3976.

Nakamura, Y., Hornsby, P. J., Casson, P., Morimoto, R., Satoh, F., Xing, Y., Kennedy, M. R., Sasano, H. & Rainey, W. E. (2009) Type 5 17beta-hydroxysteroid dehydrogenase (AKR1C3) contributes to testosterone production in the adrenal reticularis. *J Clin Endocrinol Metab,* 94**,** 2192-2198.

Noordam, C., Dhir, V., Mcnelis, J. C., Schlereth, F., Hanley, N. A., Krone, N., Smeitink, J. A., Smeets, R., Sweep, F. C., Claahsen-Van Der Grinten, H. L. & Arlt, W. (2009) Inactivating PAPSS2 mutations in a patient with premature pubarche. *N Engl J Med,* 360**,** 2310-2318.

Nowell, S. & Falany, C. N. (2006) Pharmacogenetics of human cytosolic sulfotransferases. *Oncogene,* 25**,** 1673-1678.

Orentreich, N., Brind, J. L., Rizer, R. L. & Vogelman, J. H. (1984) Age changes and sex differences in serum dehydroepiandrosterone sulfate concentrations throughout adulthood. *J Clin Endocrinol Metab,* 59**,** 551-555.

Petersen, A. M., Plomgaard, P., Fischer, C. P., Ibfelt, T., Pedersen, B. K. & Van Hall, G. (2009) Acute moderate elevation of TNF-alpha does not affect systemic and skeletal muscle protein turnover in healthy humans. *J Clin Endocrinol Metab,* 94**,** 294-299.

Pfeifer, M., Begerow, B. & Minne, H. W. (2002) Vitamin D and muscle function. *Osteoporos Int,* 13**,** 187-194.

Pfeifer, M., Begerow, B., Minne, H. W., Suppan, K., Fahrleitner-Pammer, A. & Dobnig, H. (2009) Effects of a long-term vitamin D and calcium supplementation on falls and parameters of muscle function in community-dwelling older individuals. *Osteoporos Int,* 20**,** 315-322.

Sanders, K. M., Stuart, A. L., Williamson, E. J., Simpson, J. A., Kotowicz, M. A., Young, D. & Nicholson, G. C. (2010) Annual high-dose oral vitamin D and falls and fractures in older women: a randomized controlled trial. *Jama,* 303**,** 1815-1822.

Sandri, M. (2008) Signaling in muscle atrophy and hypertrophy. *Physiology (Bethesda),* 23**,** 160-170.

Simpson, E. R. & Waterman, M. R. (1988) Regulation of the synthesis of steroidogenic enzymes in adrenal cortical cells by ACTH. *Annu Rev Physiol,* 50**,** 427-440.

Simpson, R. U., Thomas, G. A. & Arnold, A. J. (1985) Identification of 1,25-dihydroxyvitamin D3 receptors and activities in muscle. *J Biol Chem,* 260**,** 8882-8891.

Snijder, M. B., Van Schoor, N. M., Pluijm, S. M., Van Dam, R. M., Visser, M. & Lips, P. (2006) Vitamin D status in relation to one-year risk of recurrent falling in older men and women. *J Clin Endocrinol Metab,* 91**,** 2980-2985.

Stio, M., Celli, A. & Treves, C. (2002) Synergistic effect of vitamin D derivatives and retinoids on C2C12 skeletal muscle cells. *IUBMB Life,* 53**,** 175-181.

Stockton, K. A., Mengersen, K., Paratz, J. D., Kandiah, D. & Bennell, K. L. (2011) Effect of vitamin D supplementation on muscle strength: a systematic review and meta-analysis. *Osteoporos Int,* 22**,** 859-871.

Strott, C. A. (2002) Sulfonation and molecular action. *Endocr Rev,* 23**,** 703-732.

Sultan, K. R., Henkel, B., Terlou, M. & Haagsman, H. P. (2006) Quantification of hormone-induced atrophy of large myotubes from C2C12 and L6 cells: atrophy-inducible and atrophy-resistant C2C12 myotubes. *Am J Physiol Cell Physiol,* 290**,** C650-659.

Tajima, T., Fujieda, K., Kouda, N., Nakae, J. & Miller, W. L. (2001) Heterozygous mutation in the cholesterol side chain cleavage enzyme (p450scc) gene in a patient with 46,XY sex reversal and adrenal insufficiency. *J Clin Endocrinol Metab,* 86**,** 3820-3825.

Tetlow, L. C., Smith, S. J., Mawer, E. B. & Woolley, D. E. (1999) Vitamin D receptors in the rheumatoid lesion: expression by chondrocytes, macrophages, and synoviocytes. *Ann Rheum Dis,* 58**,** 118-121.

Thomae, B. A., Eckloff, B. W., Freimuth, R. R., Wieben, E. D. & Weinshilboum, R. M. (2002) Human sulfotransferase SULT2A1 pharmacogenetics: genotype-to-phenotype

studies. *Pharmacogenomics J,* 2**,** 48-56.

Van Staa, T. P., Geusens, P., Bijlsma, J. W., Leufkens, H. G. & Cooper, C. (2006) Clinical assessment of the long-term risk of fracture in patients with rheumatoid arthritis. *Arthritis Rheum,* 54**,** 3104-3112.

Verreault, R., Semba, R. D., Volpato, S., Ferrucci, L., Fried, L. P. & Guralnik, J. M. (2002) Low serum vitamin d does not predict new disability or loss of muscle strength in older women. *J Am Geriatr Soc,* 50**,** 912-917.

Wen, H. & Baker, J. F. (2011) Vitamin D, immunoregulation, and rheumatoid arthritis. *J Clin Rheumatol,* 17**,** 102-107.

Xu, Z., Wood, T. C., Adjei, A. A. & Weinshilboum, R. M. (2001) Human 3'-phosphoadenosine 5'-phosphosulfate synthetase: radiochemical enzymatic assay, biochemical properties, and hepatic variation. *Drug Metab Dispos,* 29**,** 172-178.

Xu, Z. H., Freimuth, R. R., Eckloff, B., Wieben, E. & Weinshilboum, R. M. (2002) Human 3'-phosphoadenosine 5'-phosphosulfate synthetase 2 (PAPSS2) pharmacogenetics: gene resequencing, genetic polymorphisms and functional characterization of variant allozymes. *Pharmacogenetics,* 12**,** 11-21.

Xu, Z. H., Otterness, D. M., Freimuth, R. R., Carlini, E. J., Wood, T. C., Mitchell, S., Moon, E., Kim, U. J., Xu, J. P., Siciliano, M. J. & Weinshilboum, R. M. (2000) Human 3'-phosphoadenosine 5'-phosphosulfate synthetase 1 (PAPSS1) and PAPSS2: gene cloning, characterization and chromosomal localization. *Biochem Biophys Res Commun,* 268**,** 437-444.

Yaffe, D. & Saxel, O. (1977) Serial passaging and differentiation of myogenic cells isolated from dystrophic mouse muscle. *Nature,* 270**,** 725-727.